Naval Surface Warfare Center
Carderock Division
West Bethesda, MD 20817-5700

NSWCCD-50-TR–2004/058 December 2004

Hydromechanics Department

Technical Report

EVOLVING COMPUTATIONAL CAPABILITY FOR SHIP HYDRODYNAMICS

by

JOSEPH J. GORSKI

NSWCCD-50-TR–2004/058 EVOLVING COMPUTATIONAL CAPABILITY FOR SHIP HYDRODYNAMICS

CONTENTS

ABSTRACT 1
ADMINISTRATION INFORMATION 1
INTRODUCTION 1
SHIP DESIGN PROCESS 3
RANS/CFD PROCESS 6
MONOHULL EXAMPLES 10
DTMB MODEL 5415 10
AIRCRAFT CARRIER 12
EARLY DD(X) CONCEPT 16
KRISO TANKER 18
MULTIHULLS 22
SEA SHADOW 22
TRIMARAN 25
WATERJETS 27
ATHENA 27
AWJ-21 29
BILGE KEEL PLACEMENT 31
CG-47 31
ROLL PREDICTION 33
MANEUVERING FORCES 36
YAW COMPUTATIONS 36
STEADY TURN 38
FULL-SCALE EFFECTS 39
PROPELLER INFLOW 39
WAVE HEIGHT 42
MANEUVERING FORCES 43
RANS/CFD PLAN FOR THE FUTURE 45
CONCLUSIONS 47
REFERENCES 49

FIGURES

Fig. 1 Hydrodynamics experimental support of the ship design process. 4
Fig. 2 Hydrodynamics support of the ship design process. 6
Fig. 3 CFD Process 7
Fig. 4 Structured surface grid for the DDG-51 configuration. 8
Fig. 5 Unstructured grid for the AWJ-21 waterjet. 8
Fig. 6 Computed axial velocity contours for DTMB Model 5415. 11

Fig. 7 Computed shaft and strut wakes for DTMB Model 5415. 11
Fig. 8 Computed and measured axial velocity at the propeller plane. 12
Fig. 9 Computed wave heights for Fr = 0.277. 13
Fig. 10 Surface streamlines and axial velocity contours for the model scale calculation. 14
Fig. 11 Flow field in the stern region at model scale. 14
Fig. 12 Axial velocity contours and secondary flow streamlines at X/L = 0.55. 15
Fig. 13 Computed axial velocity contours with the outboard shaft at model scale. 15
Fig. 14 Computed and measured axial velocity at the outboard propeller plane. 16
Fig. 15 Computed axial velocity contours for the advanced hull form. 17
Fig. 16 Computed and measured free surface height in the stern region. 17
Fig. 17 Axial velocities at X/L = 0.77: a) Measured, b) Computed. 18
Fig. 18 KRISO Tanker geometry. 19
Fig. 19 Surface streamlines in the stern region. 19
Fig. 20 Computed axial velocity contours in the stern of the KRISO tanker. 19
Fig. 21 Comparison of computed and measured axial velocity: a) k-e model, b) q-w model and c) full Reynolds stress model. 21
Fig. 22 Computed free surface heights for the Sea Shadow. 23
Fig. 23 Computed surface streamlines on the lower hulls and struts 24
Fig. 24 Computed axial velocity contours along the hull. 24
Fig. 25 Axial velocity contours at X/L =0.68 and 0.85. 25
Fig. 26 Computed surface pressure and streamlines for a notional trimaran 25
Fig. 27 Computed axial velocity over the front of the trimaran. 26
Fig. 28 Computed axial velocity over the stern of the trimaran. 26
Fig. 29 Axial velocity contours through the inlet of the Athena with shaft included. 27
Fig. 30 Predicted axial velocity contours at the pump inlet with a non-rotating shaft. 28
Fig. 31 Predicted axial velocity contours with a rotating shaft 28
Fig. 32 Streamlines entering the inlet trace to an upstream plane. 29
Fig. 33 Waterjet geometry for AWJ-21. 29
Fig. 34 Comparison of computed (top) and measured (bottom) axial velocities 30
Fig. 35 Computed axial velocity contours for the modified CG-47 hull. 32
Fig. 36 Modified CG-47 hull, original bilge keel position. 32
Fig. 37 Modified CG-47 hull, modified bilge keel position. 33
Fig. 38 Vortices formed along the bilge keel during a roll period. 34
Fig. 39 Computed and measured secondary velocity vectors at the end of a roll cycle; a) PIV, b) RANS computation. 35
Fig. 40 Forces for cylinder roll from Miller et al. (2002); a) zero forward speed, b) forward speed = 1.0 m/s (2kts). 35
Fig. 41 Axial velocity contours for 20 degree yaw case. 37
Fig. 42 Computed flow field for beam flow. 37
Fig. 43 Computed lateral forces. 38
Fig. 44 Axial velocity contours for Model 5415 in a turn. 39
Fig. 45 Bare hull model and full scale prediction at the propeller plane. 40
Fig. 46 Computed axial velocity contours at full scale 41
Fig. 47 Computed axial velocity at the propeller plane at full scale 41
Fig. 48 Comparison of flow at the propeller disk and average axial velocity: a) Model scale, Uave = 0.939, b) Full scale Uave = 0.972. 42

Fig. 49 Computed free surface height for Model 5415 at model and full scale. 43
Fig. 50 Computed free surface heights in the stern of Model 5415..... 43
Fig. 51 Computed axial velocity contours at X/L = 0.895: a) model scale, b) full scale. 44
Fig. 52 Surface pressure and streamlines for 20 degree yaw case; a) model scale, b) full scale. 44

THIS PAGE INTENTIONALLY LEFT BLANK

ABSTRACT

The ability to obtain flow field predictions of surface ships with Reynolds Averaged Navier-Stokes (RANS) codes has improved tremendously in the last few years. This has been a result of improvements in experience, RANS codes in general, and computer capacity. In particular, the move to parallel processing has been a major catalyst for the recent improvements and a threshold of the usefulness of RANS may well have been crossed. This is particularly significant at a time the U. S. Navy is attempting to move to high-speed ships and more operations in the littorals, both of which are driving ship designs well outside of the traditional experience and experimental data bases. A discussion of where RANS computations may be able to significantly influence the current design and analysis process for surface ships is discussed. Specific areas include: hull flow field and resistance, propulsor inflow, waterjet inlets, bilge keel and appendage alignment, roll motions, maneuvering forces, and scale effects. A number of examples are given for various configurations including: *Athena* fitted with waterjets, AWJ-21, CG-47, DDG-51, an early DD(X) concept, an aircraft carrier, and *Sea Shadow*.

ADMINISTRATION INFORMATION

The word described in this report was performed by the Propulsion and Fluid Systems Division (Code 5400) within the Hydrodynamics Department at the Naval Surface Warfare Center, Carderock Division (NSWCCD). Preparation of the report was funded by the Director for Technology and Innovation under Work Unit No. 99-5-0110-421-49.

INTRODUCTION

In "Sea Power 21" increased speed of naval vehicles is part of the vision put forth for the Navy's future. High-speed ships and craft can be significantly different than conventional monohull displacement vehicles. The Littoral Combat Ship (LCS) is envisioned as a relatively small, high-speed combatant and concepts include SWATH variants, advanced Trimarans, and semi-planning hulls such as today's fast ferries. High-speed sealift (HSSL) vehicles are much larger and the vehicles of choice tend to be monohulls, significantly more slender than current ships, or Trimarans of a similar slenderness with very small sidehulls. For high-speed vehicles a particular concern is the ability to accomplish high-speed and not severely penalize endurance. For HSSL designs in particular, high-power waterjets are deemed the propulson system needed to reach the required speeds and crucial to such designs is the integration of the hull and propulsor for better powering efficiency and reliable operation in sea conditions. Despite the U.S. Navy's rich history in pursuing high-speed craft (e.g. Clark et al., 2004) many of the designs under consideration for the future are beyond the ability of our conventional analysis techniques. This is because current ship evaluation capabilities rely heavily on model test data. For example, the available model test data is for significantly less slender hulls than many of the hulls of interest for high-speed sealift. The options are to either get data for the new hulls of interest, which can be very expensive and time consuming, or apply the current methods beyond their capability and hope for the best. Another option is to put more reliance on high end computational methods, such as Reynolds Averaged Navier-Stokes (RANS) codes, for predictions to supplement the available model test data and simpler analysis techniques.

Despite all the advances in computer power and computational techniques in the last decade one could argue that the U. S. Navy's design and analysis process for surface ships still relies heavily on the build and test approach. Although a significant amount of analysis is done, such as with the ship design program ASSET (Advanced Surface Ship Evaluation Tool) there is much empiricism to that analysis and when the hulls of interest are outside the data base the results are suspect or the data base must be expanded. An example of this is given by Fung et al.,(2001) where a series of tests were conducted for a large, high-speed surface ship to expand the ASSET powering prediction routine since the hulls of interest exceeded its boundaries. RANS computations also have their issues, such as turbulence modeling and grid generation, and care and experience are needed to get accurate answers. However, the marine industry has built itself on using simpler methods and empiricism, which in many cases provide poor predictions of the hulls and flows of interest once you are outside the traditional data base. Tremendous advances have been made in the computation of surface ship flows with RANS flow solvers in the past few years and marine designers and analysts should start taking advantage of it.

Computational capabilities are making inroads in the design processes for many vehicles outside the marine community. Aircraft design has many parallels to marine vehicle design and according to Jameson (2003) there has been a revolution in the entire engineering design process with computations playing an increasingly dominant role. Realistically, much of this computer revolution has been in the area of CAD and structural analysis. Computational fluid flow simulations have lagged these areas largely due to the fact that fluid flow is complex and hard to predict. Despite this Jameson (2003) further shows that the use of RANS codes can lead to significant improvements in drag reduction for wings and that these design improvements can be too subtle to obtain with the traditional trial and error approaches. In addition, the feasibility of combining RANS computations with optimization techniques for achieving optimum aerodynamic designs in a design process are now well established, Jameson et al.,(2004). Further, as discussed by Clark et al.,(2004) when addressing power required to achieve a given speed there is a gap between current marine and aircraft technology and the 1970 Gabrielli and Von Karman Limit Line. They further mention that the only way to close this gap for advanced marine vehicles is through improved efficiencies. Using optimization techniques, which ultimately will need to be multidisciplinary in nature, with detailed flow predictions may be the only way to gain the needed efficiencies and close this gap. Perhaps more importantly, a robust capability for full-scale predictions can provide significant risk reduction before building a final ship or making changes to an existing one.

RANS has been demonstrated to be generally applicable to many types of hull forms. This has been demonstrated numerous times in the literature and NSWCCD has been at the forefront of applying RANS to complex surface ship flow predictions. In fact, the author has written various reviews on the subject, Gorski (2001, 2002a). The improving capability has been partly due to the maturing software as well as the advances that have been possible with increasingly faster computers. With advances in both areas it is now possible to compute the flow field of a surface ship with some degree of confidence. It is also not unreasonable to expect computer power increases to continue to follow Moore's law, where computer power doubles every 18 months, for approximately the next 25 years. This is when it is expected computer hardware will reach the limits at the atomic scale, but will provide computer processing speeds on the order of a million times greater than today (Frank, 2002). This is a phenomenal increase in power that should be available to many of today's young engineers. It is probably difficult to even imagine how this increase in computational power will change the way marine vehicles are

designed and analysed in the future. One would also expect that high-end computational techniques, such as RANS, will become more of a design/analysis tool and with less reliance on the current build and test mind set. The experiments should become more high-end and detailed themselves to support this change in paradigm. However, evaluating the changes in our design processes over the last decades it is also possible to imagine it might not change much in the foreseeable future. This is because we constantly pursue simpler inviscid methods, which employ less physics, combined with experimental data for much of the design and analysis currently done. The correct approach seems to be to use the mix of tools we have at our disposal and constantly attempt to capitalize on the latest developments in better predictive capability in our design/analysis processes. To do this often requires the regular use of these tools and a proposed plan is described in a latter section.

This report attempts to encapsulate where current RANS technology is for surface ship predictions and where it might be most appropriate to bring into the design and analysis process. Specific areas include: hull flow field and resistance, propulsor inflow, waterjet inlets, bilge keel and appendage alignment, roll motions, maneuvering forces, and scale effects.

SHIP DESIGN PROCESS

The design and analysis of surface ships is still largely compartmental in nature and the areas of resistance, propulsion, maneuvering and seakeeping are often performed independently of one another. Hydrodynamics support of a design cycle might typically be shown as a largely experimental process, as in Fig. 1, and also usually flows counterclockwise starting from resistance and powering. However, much analysis is often done as part of a design cycle, albeit with much simpler codes than RANS. Mission requirements drive the ship design process and codes such as ASSET (Sheridan et al., 1984) are used during the very early design stage to calculate and balance ship characteristics. Such codes allow one to quickly evaluate the design space and do trade-off studies to achieve the best solution for the required mission. These codes run very quickly, but the estimates are based on simple calculations and the heavy reliance on historical data. As already mentioned the data base needs to be expanded to have confidence for novel hull shapes. The next step is often more detailed hull design including resistance studies. This is often done with codes such as TSD0 (Metcalf et al., 2004), which combines a mix of analysis techniques, such as a potential flow code for the wave drag, the ITTC 1957 ship-model correlation line for friction drag, and modified approximations from Hoerner (1965) for the form drag and transom drag developed from observed changes on a number of shapes. Panel methods can provide the wave resistance, but estimates are still needed for the frictional resistance and form drag. These are obvious areas RANS can contribute as well as providing more detail flow physics of the hull chosen, such as possible flow separation. The propulsor is often treated separately from the hull with the design based largely on powering requirements and propulsor inflow. Although this has worked well for conventional designs it is probably an oversimplification for integrated propulsor/hull concepts and waterjets in general.

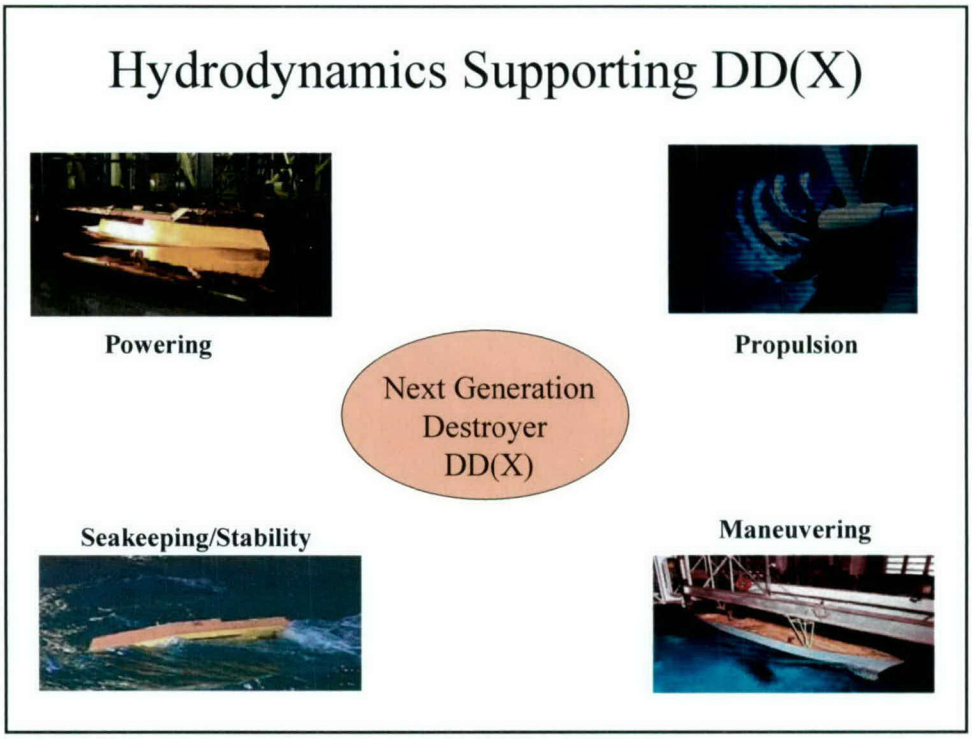

Fig. 1 Hydrodynamics experimental support of the ship design process.

RANS can both provide the propulsor inflow and the interaction effects between the hull and propulsor for integrated designs. In fact, the majority of surface ship RANS efforts have focused on straight ahead flow related to resistance and powering. For naval vehicles the flow into the propellers is significantly influenced by the upstream hull form, Gorski (2001). This includes the boundary layer generated on the hull as well as any vortical flow that may form such as that from the bow/sonar dome or bilges. Additionally, wakes are formed from upstream bilge keels, shafts, and supporting struts. Of particular significance for many naval combatants are the shaft and strut wakes, which are immediately upstream of the propellers. RANS codes provide a means of predicting such flow fields as has been demonstrated by Gorski et al., (2004) and also provide an ideal means of obtaining inflow to waterjets, Ebert et al., (2003). The same calculations can also be used for appendage alignment as discussed below.

Ship motion prediction programs such as FREDYN (e.g. de Kat and Paulling, 1989) have matured to the point where they are routinely used for predicting ship motions in severe seas. Such codes are quite sophisticated and include a variety of individual forces including: Froude-Krylov, radiation, diffraction, rudder and appendages, propeller, maneuvering and viscous. Some of these forces are difficult to predict computationally, as discussed by Beck and Reed (2000), even for the limited case of forward speed in waves. Consequently, a hierarchy of models, which has evolved for the prediction of the individual forces, have been used with varying degrees of success. Despite the limitations of predictive techniques there has been significant success in predicting the large amplitude motions of particular hull forms. Part of the reason for this is that the buoyancy and Froude-Krylov forces, which are relatively straightforward to predict, dominate in large amplitude motions. Another reason such codes can be used with confidence for certain hull forms is their reliance on experimental data for many of the individual force components. This is fine when computing flows for hull forms where the

needed experimental data are available. They can also work well for new hull forms where the Froude-Krylov forces dominate and the empirically based approximations are reasonable. However, when applied to a new hull form, or in situations where Froude-Krylov forces may not dominate, one cannot be sure how such methods will perform until they are compared with experimental data. This limits to what extent the codes can be trusted or used in design cycles, as the various forces are included through linear superposition and cannot account for highly complicated flow physics where higher order effects and interactions among the various force contributors becomes significant. Getting such details can be very difficult, time consuming and expensive. Trade-offs must be made between an engineering useful solution and a highly accurate solution, which may or may not be attainable. This is not a criticism of the current large amplitude prediction codes. They are very necessary as there is no acceptable alternative at the present time. However, because capsize is such a catastrophic event any potential improvement in predictive capability that can be achieved should be evaluated. Maneuvering forces are often included in such codes using empirical data or simple analytic techniques.

Maneuvering and seakeeping is a relatively new area for RANS calculations. RANS codes offer the possibility of computing more of the physics directly and are being pursued for submarine (Taylor et al., 1998), aircraft (Schütte et al., 2002) and surface ship (Kim, 2001) maneuvering simulations. Such computations are currently much too slow for realistic maneuvering and seakeeping simulations and will be so in the foreseeable future. However, RANS may be able to contribute where no experimental data exists, which can be extremely useful. Roll motion is an obvious area where viscous effects are important and the models based on empirical data-bases have potential to break down as new hulls, such as tumblehomes, come under consideration. RANS has already demonstrated it can be used to properly predict bilge keel forces for simple geometries (Miller et al., 2002). Maneuvering forces is another area RANS can contribute. Forces on low aspect appendages can readily be computed with RANS (e.g. Gorski and Buley, 1998), but perhaps more importantly is the possibility to compute the hull forces and interaction between the hull and appendages. An example of the complexity of hull flow fields at angles of yaw is demonstrated below. So although RANS cannot be used to solve the seakeeping problem directly it is worthwhile to evaluate where RANS calculations can contribute to the prediction and understanding of ship motions, Gorski (2002b).

There are always issues with using the experimental data at model scale in all of the above areas and extending it to full scale. This is usually done with correlation allowances and other ad hoc methods for describing the way the model behaves vice how the eventual full scale ship behaves. This can incur tremendous risk at full scale for new classes of ships. Full scale RANS computations are becoming more routine and differences are seen in the flow field and forces from model to full scale as demonstrated in this report. Evaluating such effects with RANS codes, and the potential risk mitigation they can provide when going to full scale, may be on of the most important reasons to pursue RANS in the near future.

Because of the likely move to integrated designs in the future all aspects of ship design will probably be evaluated much earlier in a design cycle when it is generally most cost effective to change a design. At the early design phase computations are very attractive and an era is evolving where a large number of computational studies are performed for new hull forms, in some sense replacing the series tests of old, and model testing is done for the final geometry. For radical new hull forms there will be limited confidence in largely empirical based methods and more exact computational methods are desired. This will involve a hierarchy of methods from

simple analysis to highly complex RANS calculations and perhaps even more sophisticated simulations such as Large Eddy Simulations in the future. Rood (2000) discusses how RANS codes are starting to revolutionize ship hydrodynamics design and evaluation procedures from traditional towing tank methods to computational based methods. Examples of how RANS calculations have been used to influence submarine (Gorski and Coleman, 2002) and surface ship (Gorski et al., 2002) designs already exist and it is anticipated they will have more impact in the future. An alternative design process is shown in Fig. 2 where representative computational codes are placed in the design process. Again the flow is largely counterclockwise starting from hull design. Ultimately there will need to be interactions between all of the various components and other areas such as structures to achieve truly revolutionary designs.

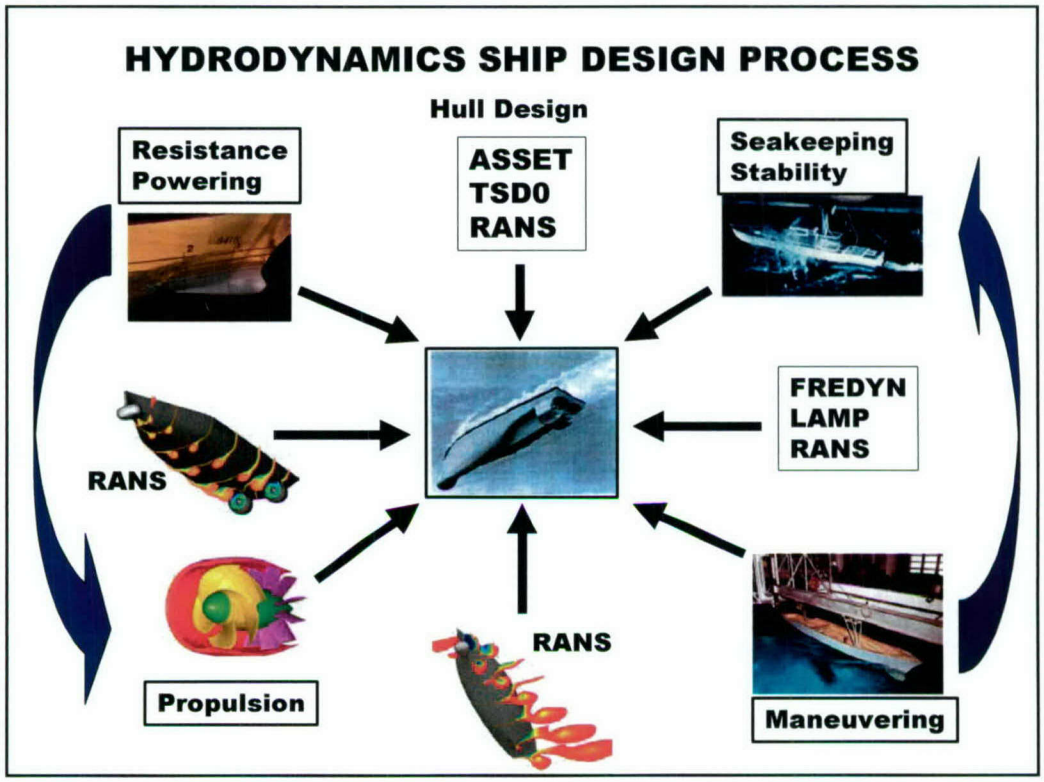

Fig. 2 Hydrodynamics support of the ship design process.

RANS/CFD PROCESS

It should be pointed out that to perform good flow calculations is not simply a matter of turning on a particular piece of software, particularly for complicated geometries or flows. The computations, with either RANS or other flow solvers, involve a process not unlike that of doing a model experiment. A test of whether a particular code can predict certain physics is dependent on all pieces of this process. An idea of what this process is like is shown in Fig. 3. The validation of the calculation depends on all of the steps in the process. A problem with any one of them can lead to differences in the computed and real flow physics.

The process starts with the satisfactory specification of the actual geometry. Details, such as ensuring there are no gaps in the geometry and trimming surfaces, must be taken care of

before the geometry can be used easily with grid generation software. For the actual definition of the geometry, a single B-spline surface for each component is preferred. B-splines can model the most complex shapes and provide smooth, continuous definition with well-behaved intersections. In the IGES format, they can be transferred between most CAD and grid generation software packages.

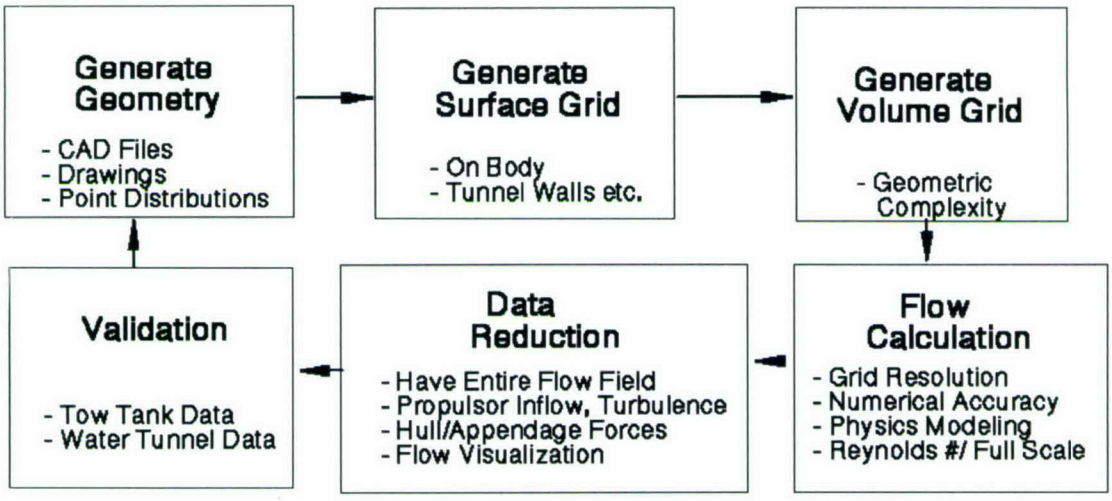

Fig. 3 CFD Process.

When generating the computational grid, a surface grid must first be generated on the body and all surrounding boundaries where boundary conditions are imposed. This surface grid breaks up the smooth B-spline surface into discrete points and one must make sure the grid conforms to the actual geometry. Additionally, these surface grids must be clustered in areas of high geometry gradients or where the flow is expected to change rapidly to help provide accurate predictions. It is very important in shaping or sculpting a geometry that enough attention to detail is done so that changes in the actual geometry are properly represented in the discretized geometry. A volume grid is next generated providing discrete points in the entire flow domain where the Navier-Stokes equations are solved. A computed solution can only be as good as the grid on which it is computed. If there are high gradients in the flow, such as in boundary layers, wakes and vortices, it is necessary to have enough grid points in these areas to resolve them. If enough grid points are not present the computation will diffuse these high gradients. Once a flow feature is diffused in this, or any other way, its impact and interaction on the surrounding and downstream flow cannot be predicted accurately. For viscous calculations, and drag comparisons in particular (Gorski, 1998) attention must be paid to these details to insure one is predicting flow differences due to actual geometry changes and not differences due to computational changes. In practice it is sometimes difficult to achieve good grid quality, a sensible amount of time spent, and a practical grid size all at the same time. Most of the flow calculations in this report have been done using structured grids, which have been the standard for many years. For complicated geometry, such as including shafts and struts, a good structured grid can become very complicated in its own right. An example of a structured grid on the surface for the stern of DTMB Model 5415 is shown in Fig. 4. Once generated, such grids can provide very good results, as demonstrated later, but they can be time consuming to create. Progress with unstructured grids has greatly simplified the grid generation process and it has

been demonstrated that the same accuracy can be obtained with unstructured grids as structured grids (e.g. Dailey et al., 2003). An example of the unstructured grid used for computing the flow field of the AWJ-21 waterjet configuration is shown in Fig. 5. This has all the complications of the previous structured grid, but took significantly less time to generate. In addition, such unstructured grid technologies lay the foundation for evolving grid adaption techniques, which will more easily allow grid points to be placed in important areas of the flow.

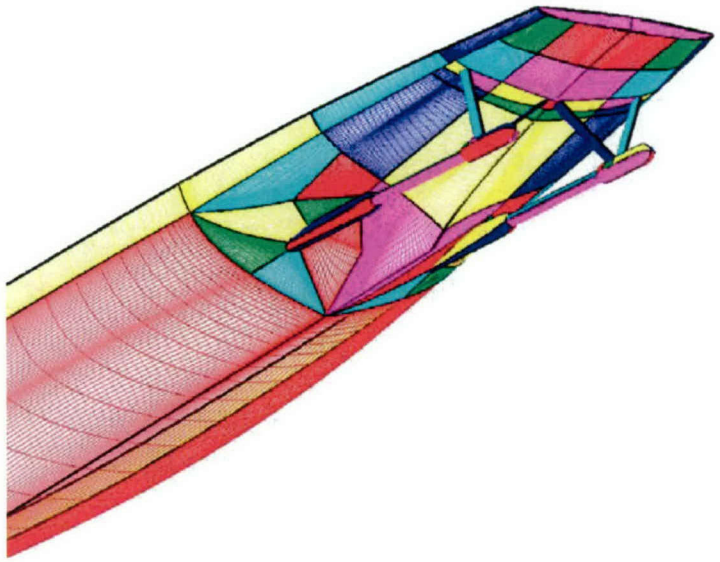

Fig. 4 Structured surface grid for the DDG-51 configuration.

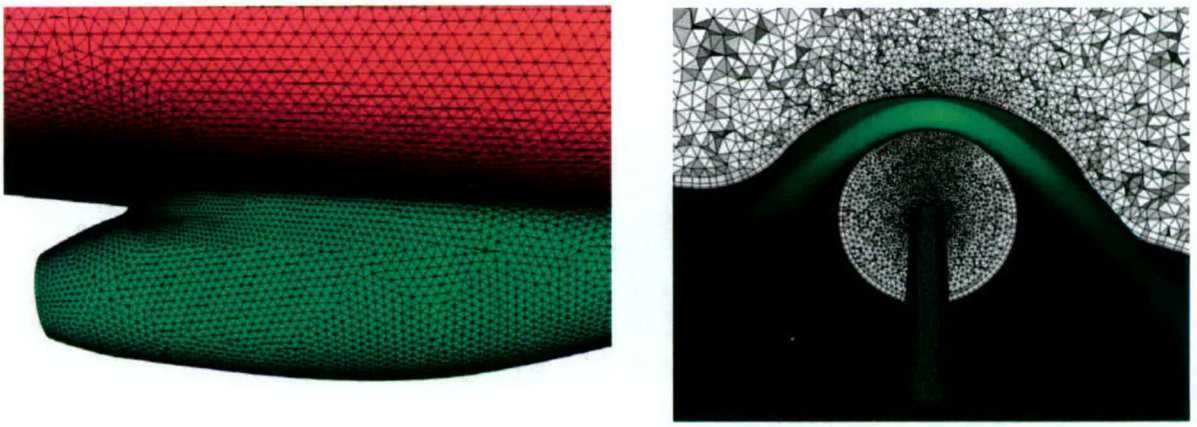

Fig. 5 Unstructured grid for the AWJ-21 waterjet.

Obviously flow solutions also depend on the RANS code used. Many of the calculations shown here are obtained solving the incompressible Reynolds Averaged Navier-Stokes equations using the Mississippi State University code UNCLE (Taylor, et al., 1991,1995). Much success has been achieved with this code and it was an important tool when its parallel version came out, Taylor et al., (1998). An important factor in being able to compute and evaluate the hull modifications and operating conditions of interest has been the implementation of parallel computational capability. To run in parallel the computational grid is decomposed into various

blocks, which are sent to different processors. Load balancing is obtained by making the blocks as equally sized as possible. Although many of the computations shown here have been performed with the UNCLE code the CFD area is rapidly evolving to keep pace with computer and numerical advances. Various RANS codes are now available both commercially and from university sources. These codes have their individual strengths and weaknesses in terms of applicability, usability, speed, grid options, turbulence modeling options and free surface capability to name but a few of the parameters. Consequently, a number of CFD/RANS codes are used at NSWCCD where we try to use the correct code for each problem. Some of these codes are the unstructured U2NCLE code (e.g. Hyams et al., 2000), the CFDSHIP-IOWA code (e.g. Paterson et al.,2000), and the commercial codes COMET (e.g. Perić, 1994) and FLUENT (e.g. Kim, 2000).

Another issue affecting accuracy is the turbulence modeling used. Two-equation models have become the standard for practical applications. In the current studies k - ε and q - ω models are most often used. However, the advantage of having a number of codes to use is also the ability to try a variety of turbulence models if necessary. The two-equation models are often adequate for many applications of interest. For highly complicated flows where great accuracy is desired it is sometimes necessary to use more elaborate turbulence models, such as the Reynolds stress model. One such case is tanker flows where the very strong vortical flow at the stern requires a more sophisticated model to predict it accurately. An example of this is shown later for the KVLCC2 tanker. For all of the computations the equations are solved right to the wall without the use of wall functions. For solving directly to the wall it is generally preferable to have the first point off of the wall well within the viscous sub-layer and a value of y^+ around 1 is the typical goal. Computations at higher Reynolds numbers requires the relative distance of the first point off of the wall to become smaller to maintain this criterion.

The free surface prediction has been an issue with such flow solvers. One approximation has been to use the double-model approximation, which greatly simplifies the computation. The double-model condition simulates the flow about the "double body" formed by reflecting the hull about the undisturbed water level. The undisturbed water level is treated as a symmetry plane where the vertical velocity is set to zero. The double-model condition is a good approximation to a free-surface condition if the speed of the hull is low or if the flow region of interest is sufficiently far from the water surface. The shape of the water surface is computed subject to the conditions that the flow is tangential to this surface and that the pressure is atmospheric. The linearized free-surface approximation can also be used where these conditions are applied at the undisturbed water level rather than at the actual computed free-surface level. This option avoids the complication of having to move the grid to conform to the free-surface shape as it is computed. Similar to the double-model approximation, the linearized assumption is a good approximation if the wave slopes are small or if the flow region of interest is sufficiently far from the water surface. Comparison of results obtained with the double-model condition with those obtained with the linearized free-surface condition shows that for many purposes, such as the propeller inflow, use of the double-model condition is quite sufficient. However, to compute more complicated free surface effects the actual free surface needs to be computed.

The dominant method of predicting the free surface has been to use the kinematic condition that the water surface acts like a material boundary. This bounds the domain and the flow field is solved for the water portion of the problem with a dynamic boundary condition applied at the water surface for the Navier-Stokes equations. Usually only inviscid boundary

conditions are applied at the water surface despite the use of a viscous flow solver, but this should have little influence on the large scale waves. Because the water surface is now a boundary to the domain a grid must be generated in the domain using the hull and water surface as its boundaries. This method can work very well, but the approach can be problematic. Once the free surface starts changing the grid must adjust, usually along existing grid lines, to accommodate the new free surface height. Here good grid quality is easily lost and if changes become too large the grids often become too highly skewed for stable running of the RANS code. An alternative is capturing methods, which are receiving increased attention in ship hydrodynamics. These include the level set and volume of fluid methods for ship free surface calculations. With these methods both the air and water are computed with a discontinuous jump in density and viscosity allowed across the interface between them. These methods are becoming available both in the university and commercial codes already mentioned. The results are also promising for motion prediction without the difficulties associated with grids evolving to conform to the free surface. The above methods can handle very complex interfaces, including wave breaking, and should allow RANS codes to be more easily used for maneuvering and seakeeping calculations in the future.

Although there are issues involved in getting accurate flow computations with RANS codes the build-up in experience and capability has lead to the ability to compute the flow fields of many real hull shapes of naval interest. A major advantage of such codes is the generality they inherently have to be applied to many different configurations. To demonstrate this a number of computed flow fields for different hulls are now shown.

MONOHULL EXAMPLES

Many of the computations to date have been for monohulls. However, even here a variety of examples are available. To demonstrate some of the capabilities of RANS codes computational results are shown for DTMB Model 5415, which is an early version of DDG-51, an aircraft carrier, one of the early DD(X) concepts with a tumblehome design and wave piercing bow and a tanker configuration. These examples demonstrate a wide range of applicability. The bare hull results showing how significantly the flow can change due to the particular hull configuration. In addition, the impact shafts and struts make on the propeller inflow are also shown. The results here are all for model scale and straight ahead flow conditions. Later sections address scale effects and angle of attack.

DTMB MODEL 5415

Perhaps the most extensively measured and computed naval combatant is the bare hull version of DTMB Model 5415 (Ratcliffe, 1998), and its geosyms, which is an early version of DDG-51. Tow tank data include: resistance, sinkage and trim, wave profiles, near- and far-field wave elevations, mean flow (taken with pitot probe and LDV), and turbulence data. A fully appended model was also tested at DTMB including shafts, struts, and rudders. For Model 5415 the flow near the bow has a large downward component resulting in the creation of a bow dome vortex. This disturbance grows as it is convected downstream and combines with the hull boundary layer. This vortex may also be enhanced by the general downward and inward flow over the forward bilge. For the bare hull configuration this is the major flow disturbance into the propeller plane. A computation showing axial velocity contours along the hull is shown in Fig. 6. For this calculation the model is run straight ahead at a speed of 4.0 knots for a

corresponding model scale Reynolds number of 12 million, based on length, and Froude number of 0.277. The decrease in draft at the stern accentuates this wake as the propeller plane is approached.

Fig. 6 Computed axial velocity contours for DTMB Model 5415.

When shafts and struts are included, the upward and inward flow due to the decrease in draft and width of the hull, results in a shaft wake above the shaft and beneath the hull. The bow dome vortex still persists at the propeller plane. However, the shaft and strut wakes combine with the bow dome vortex and the hull boundary layer to further complicate the flow into the propeller plane, Fig. 7.

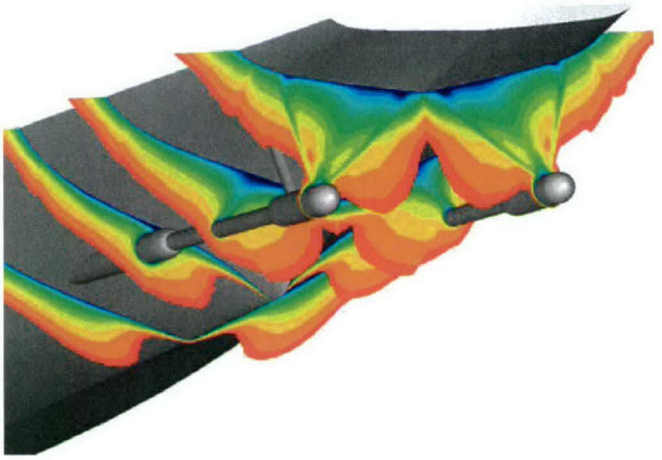

Fig. 7 Computed shaft and strut wakes for DTMB Model 5415.

A comparison of the calculated axial velocity at the propeller plane with the measured data of Chesnakas is shown in Fig. 8. This LDV data were obtained near the propeller plane without the propeller operating. The calculation captures the angled v-shaped wake formed from the combination of the bow dome vortex, hull boundary layer and the shaft wake. The calculation also shows the presence of strut wakes in the flow field. The struts' wakes tend to sharpen the wake's v-shape. This feature is missing in the experimental data, probably because

of the coarseness of the measurement data locations. To evaluate the effect of the struts on the propeller inflow, a calculation was also performed without the struts. The results indicate that the struts tend to widen the wake immediately above the shaft. It appears that the wake of the shaft joins with the inboard strut wake, which is more in the cross-flow direction, thickening the overall disturbance. However, the comparison with the shaft alone demonstrates that the shaft wake dominates significantly over the strut wakes as long as the struts are aligned with the flow. Further details can be found in Gorski et al., (2004).

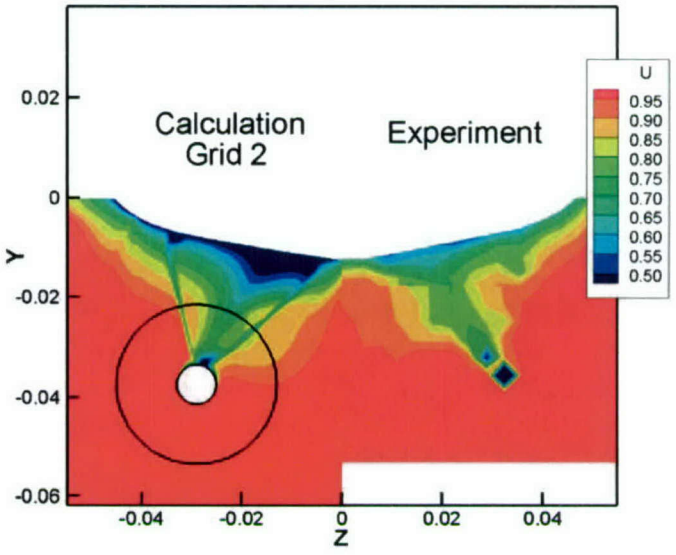

Fig. 8 Computed and measured axial velocity at the propeller plane.

AIRCRAFT CARRIER

A number of computations have also been performed for an aircraft carrier, Gorski et al., (2004) with the major features including a bulbous bow, a transom stern, bilge keels, a docking skeg and propeller shafts. Unlike the destroyer the carrier has a large flat section on the bottom. This large flat section along with the vertical wall sided hull leads to a more pronounced bilge over the forward part of the hull that can produce more significant bilge vortices. Consequently, the bare hull flow generated by the carrier configuration such can be quite different than a destroyer.

For the computations the hull is sunk and trimmed appropriately, based on experimentally obtained values, and run at a model scale Reynolds numbers, based on hull length, of 35×10^6. Calculations are for a Froude number of 0.277 with linearized free surface boundary conditions. The computed free surface elevations for the model scale prediction are shown in Fig. 9. This computed free surface height along the hull agrees well with

experimentally obtained data[1] also shown in Fig. 9. The inclusion of the outboard shaft has no noticeable impact on the computed free surface heights.

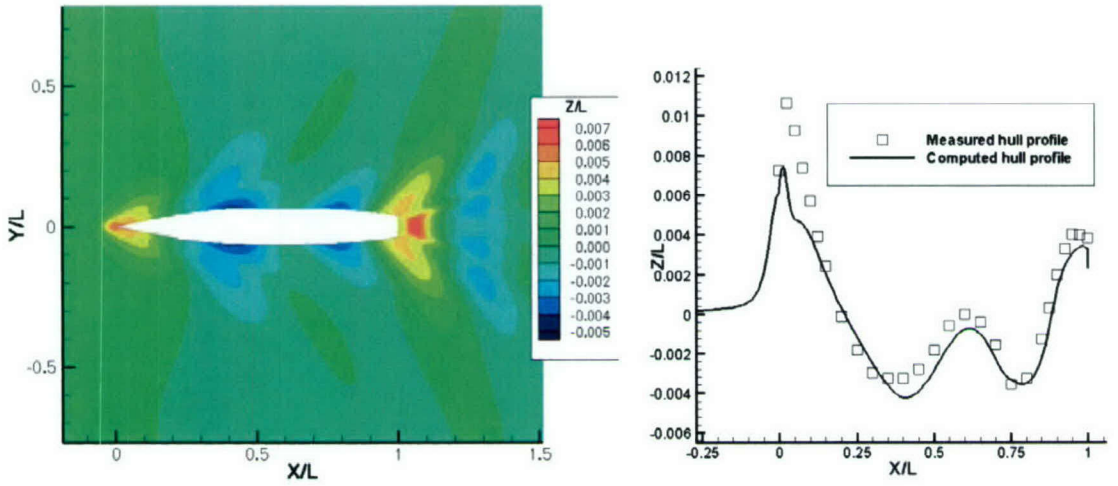

Fig. 9 Computed wave heights for Fr = 0.277.

Computed surface streamlines and axial velocity contours at various locations along the length of the hull are shown in Fig. 10. It can be seen that the boundary layers are relatively thin, even at model scale, over most of the hull. Flow is generally downward over the forward part of the hull and then runs axially along the hull mid-section. The downward flow over the bow area creates a vortex over the bow dome that convects downstream along the hull centerline. However, this vortex is rather weak and has negligible impact on the hull boundary layer midway down the length of the hull. The hull has rather sharp bilges and a bilge vortex is forming toward the stern, which also interacts with the bilge keel. This vortex travels downstream and is the dominant feature in the propeller plane area as seen in Fig. 11. As shown, the wake retains much of the hull shape as it propagates downstream and takes on a very flat behavior at the stern on the underside except for the skeg wake. Due to the free surface interaction, there is a downward component of the flow at the stern, and then an upward flow toward the transom.

[1] Experimental data provided courtesy of Code 5200, Naval Surface Warfare Center, Carderock Division, West Bethesda, MD.

Fig. 10 Surface streamlines and axial velocity contours for the model scale calculation.

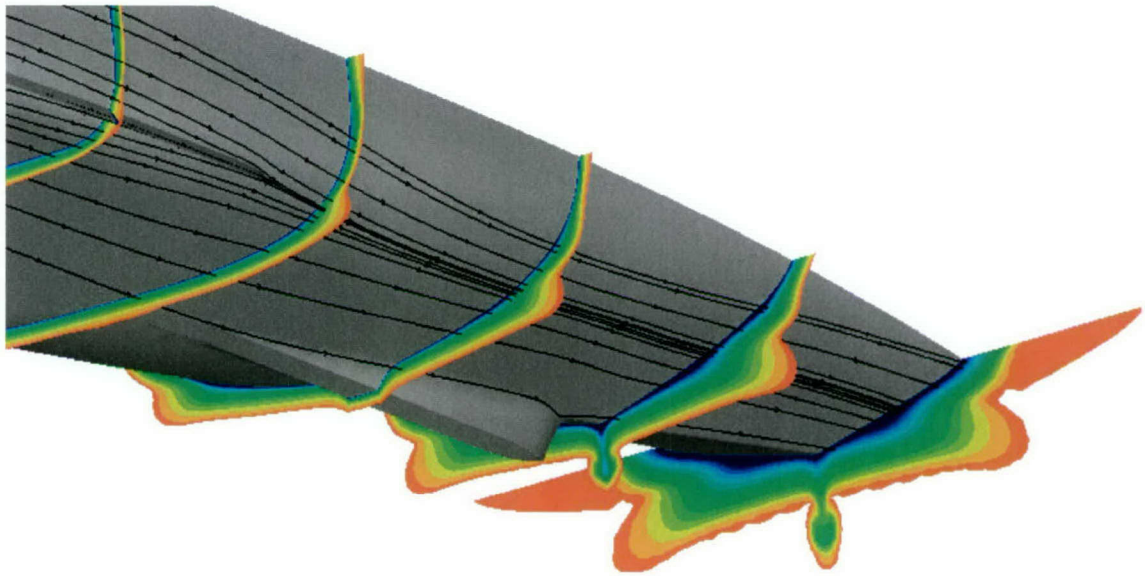

Fig. 11 Flow field in the stern region at model scale.

It can be seen in a cross section at X/L = 0.55, Fig. 12, that the generally outward and upward flow around the bilge creates the downstream vortical flow and it appears the bilge keel impacts this. This bilge/bilge keel vortex is the dominant flow into the propeller plane at model scale when the shafts and struts are not present.

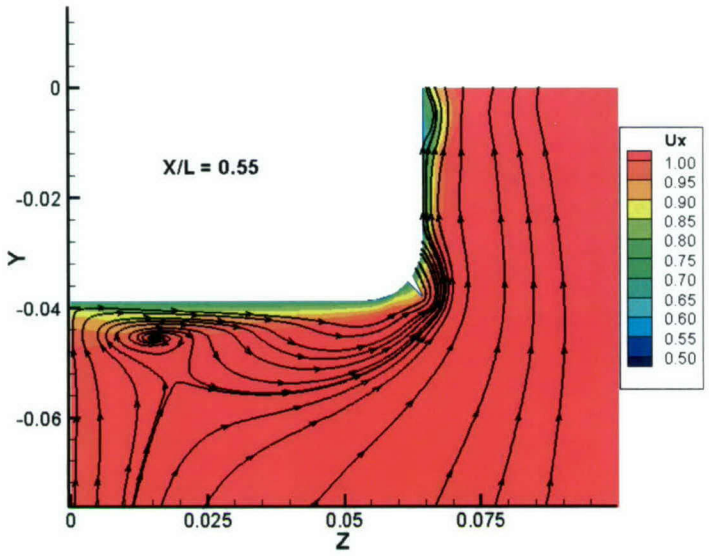

Fig. 12 Axial velocity contours and secondary flow streamlines at X/L = 0.55.

Calculations are also performed which include the outboard shaft. The inboard shaft is not modeled nor the supporting struts for the outboard shaft. Computed axial velocity contours near the stern of this hull are shown in Fig. 13. It is seen that the bilge/bilge keel vortex flow that is the dominant feature at the stern for the bare hull configuration flows directly into the outboard shaft. The shaft changes this flow significantly creating an additional wake deficit in the outboard propeller disk. Also seen in Fig. 13 is a noticeable effect on the flow downstream of the outboard propeller shaft, due to the interaction of the bilge vortex and shaft.

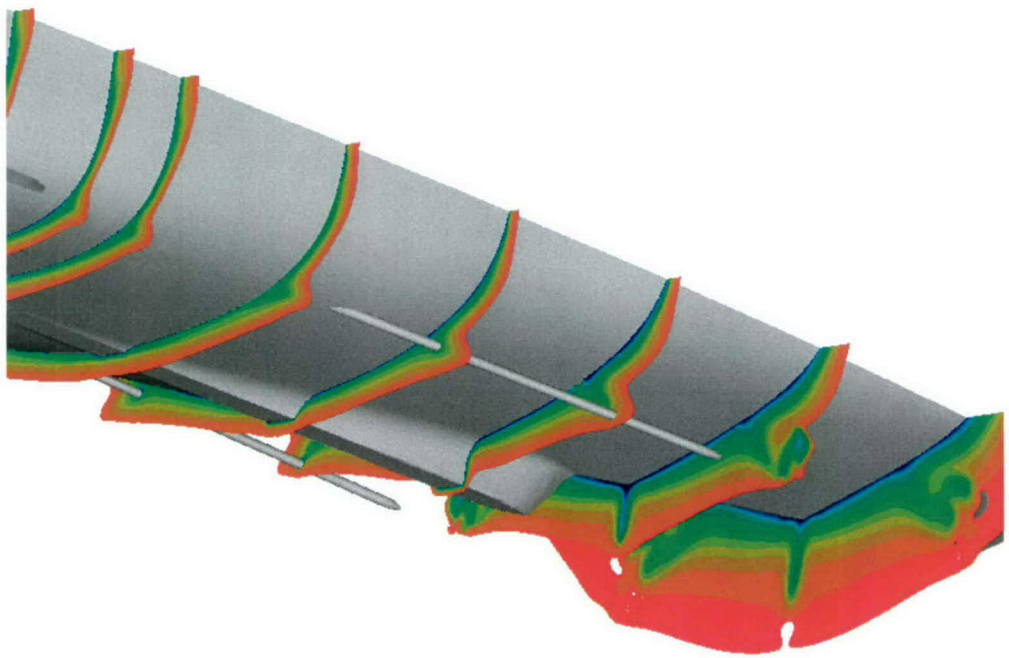

Fig. 13 Computed axial velocity contours with the outboard shaft at model scale.

A comparison of axial velocity at the outboard propeller disk between experiment[2], the bare hull computation, and this computation with the shaft shows the significance of the shaft presence, which is a dominant feature into the propeller disk. This is demonstrated in Fig. 14. The bare hull flow has none of the sharp wake-like velocity deficit. The computation with the shaft agrees well with the measured data, which also has the wake-like deficit. The measured data has a somewhat wider wake, which is likely due to the struts in the experiment. The supporting struts were not included in this calculation which may account for some of the differences. Full details of the computation, as well as scale, propulsion, and shaft rotation effects can be found in Gorski et al., (2004).

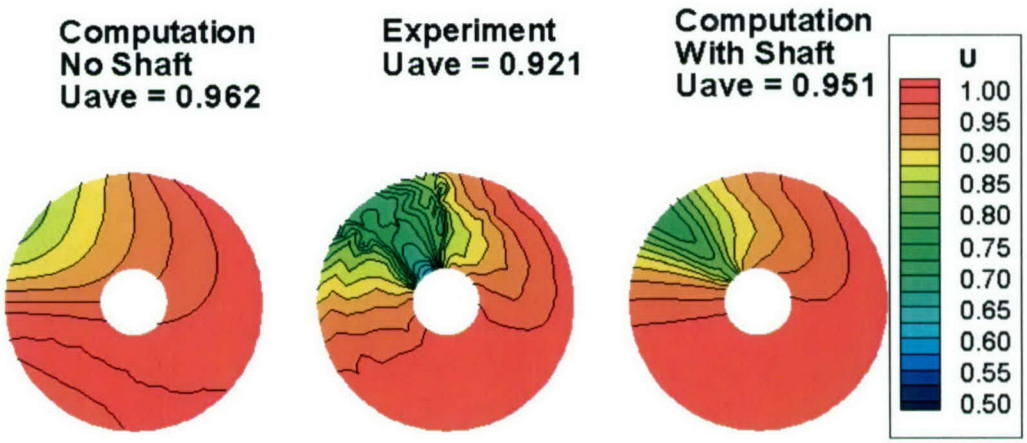

Fig. 14 Computed and measured axial velocity at the outboard propeller plane.

EARLY DD(X) CONCEPT

Perhaps a catalyst for much of the current success with RANS codes was the ONR Surface Combatant Accelerated Hydrodynamics S&T Initiative. The objective of this effort was to apply verified, validated, and benchmarked computational ship hydrodynamics to the exploration of innovative propulsor/hull concepts and to develop tools and concepts for technology options for DD(X) and beyond. The desire is to use these computational tools to help evaluate 'out of the box' designs so a large experimental program is not needed. To adequately test the computational tools at that time a complex surface ship geometry with strong propulsor/hull interaction was desired. Since no traditional model existed for this hull form it needed to be designed, built, and tested as part of the effort. The hull form studied is a tumblehome design with a wave piercing bow and ducted propulsors and a variety of computations and experiments performed on it. Details of how the use of RANS calculations contributed in the actual design cycle, where 5 different variants were computed and details of the hull shape were changed based on the predicted results, can be found in Gorski et al., (2002).

[2] Experimental data provided courtesy of Code 5200, Naval Surface Warfare Center, Carderock Division, West Bethesda, MD.

The final tested geometry with computed axial velocity contours at several longitudinal positions along the body is shown in Fig. 15. It is clearly evident that the vortical structures from the bow dome flow along the hull and enter directly into the propulsors.

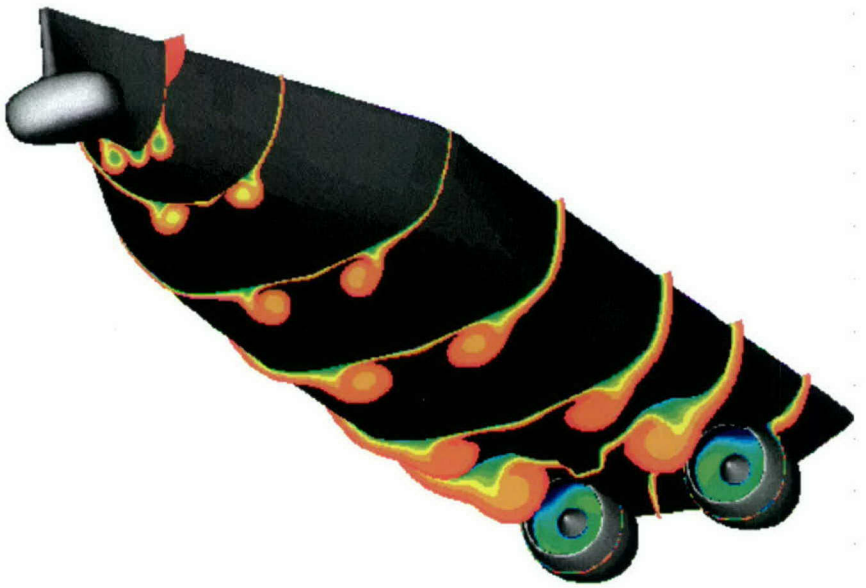

Fig. 15 Computed axial velocity contours for the advanced hull form.

These calculations are performed at model scale corresponding to a Reynolds number, based on model speed and length, of 15.44e+06 and a Froude number of 0.232. Body force terms are included for propulsion approximately halfway through the propulsor in the streamwise direction, but the hub is included directly in the computation. Comparisons with free surface heights measured immediately downstream of the hull are shown in Fig. 16 with the computed wave height on top and the measured wave height on the bottom. The data show a rooster tail forming immediately aft of the hull with a trough downstream of that. The computed solution captures the flow extremely well.

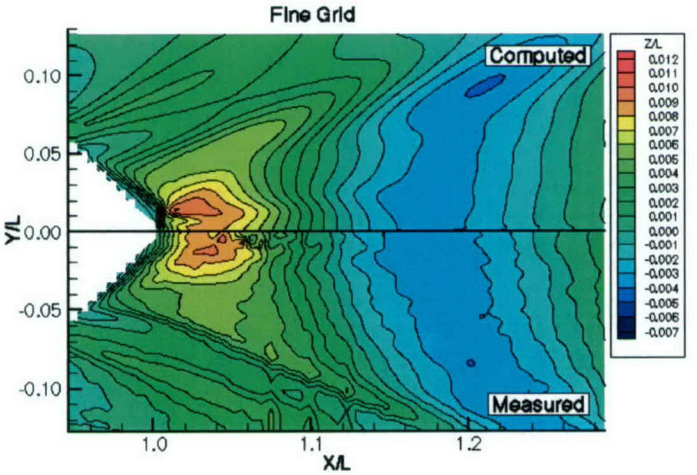

Fig. 16 Computed and measured free surface height in the stern region.

The measured and computed axial and secondary flow velocity at X/L = 0.77 is shown in Fig. 17, which is in the scooped out area just upstream of the propulsor. This data were taken with a LDV system and axial velocity contours are shown with secondary flow vectors. The dominant feature is the vortex, which is generated at the bow dome. The most apparent difference between the computed and measured data is a slight shift of the vortex location. This shift is probably due to the computed vortex not being as strong as the actual vortex, which can be inferred from the secondary flow vectors. However, the agreement is very good and the predictions are accurate enough to provide cavitation estimates for the propulsor. Details of how the various geometries changed the flow field as well as a grid resolution study are in Gorski et al.,(2002).

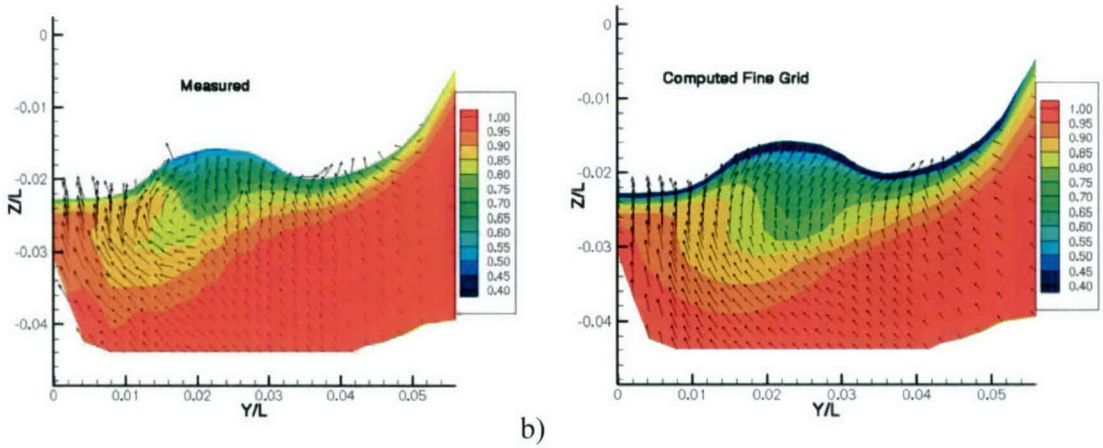

a) b)

Fig. 17 Axial velocities at X/L = 0.77: a) Measured, b) Computed.

KRISO TANKER

Computations have also been performed for the Korean Institute of Ships and Ocean Engineering (KRISO) 300K very large crude oil carrier (VLCC). Although tanker flows are not necessarily directly applicable to Navy combatants and high speed craft the hull form is for a modern tanker with bow bulb and stern, Fig. 18. The flat bottom with vertical sides is similar to an aircraft carrier and has a somewhat similar flow. The stern, however, leads to flow that can be very complex with the generation of strong longitudinal vortices and the potential for axial separation at the stern. The complexity of this stern flow can be seen from the computed surface streamlines shown in Fig. 19. There is a generally upward flow near the stern as expected, but the complicated stern shape leads to some downward flow right at the stern and a limiting streamline near the keel is formed. From the computed axial velocity shown in Fig. 20 it can be seen that just upstream of the stern there is typical boundary layer flow with a bilge vortex. This is similar in some respects to the carrier flow field except the hull shaping causes the bilge vortex to convect toward the waterline. Downstream of this in the very stern region a very strong bilge vortex is formed that creates a distinctive hook pattern in the axial velocity contours at the propeller plane. This stern bilge vortex causes the axial velocity to move outboard away from the hull along the centerline, which interacts with the generally upward flow of the free stream velocity around it to create the distinct hook shape. It is interesting to note that the Model 5415 flow at the stern is opposite of this with the axial velocity moving inboard at the centerline creating a distinctly different flow pattern as shown previously, Fig. 6.

Fig. 18 KRISO Tanker geometry.

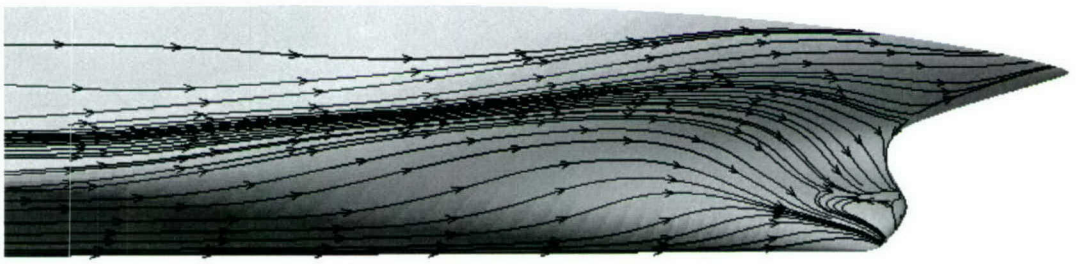

Fig. 19 Surface streamlines in the stern region.

Fig. 20 Computed axial velocity contours in the stern of the KRISO tanker.

The tanker geometry was chosen as a CFD validation test case for the Gothenburg 2000 (Larsson et al., 2003) workshop on ship flows. The experimental data used at the workshop is from a double hull model measured by Van et al., (1999) in a wind tunnel at a Reynolds number of 4.6 million. Accurately predicting the strong bilge vortex at the stern has proven to be a challenge for RANS codes and their turbulence models in particular. For predicting largely boundary layer flows the simpler two-equation models seem more than adequate. However, when predicting complex flows with secondary separation they may be inadequate. The k-e model is too dissipative, even with highly refined grids. The results from the workshop seemed to indicate full Reynolds stress models are necessary for accurately predicting this complex flow at the stern. Deng and Visonneau (2000) used a number of models and showed the best results with a full Reynolds stress model. They concluded that while simpler nonlinear models could do better for this flow than the basic two-equation models, only solving the full Reynolds stress transport equations would accurately predict this strong vortex flow since the local equilibrium assumption, which the simpler models are based on, is not valid. Perhaps the best results for this case were presented by Kim (2000), who also used full Reynolds stress turbulence models with FLUENT. An interesting side note is that Kim did not solve the equations down to the wall, but used wall functions. Computations obtained here also indicate the higher order turbulence models are necessary for predicting the stern flow accurately. Shown in Fig. 21 is a series of computations with the k-e, q-w and a full Reynolds stress turbulence model as compared to the experimental data of Van et al., (1999) at the propeller plane. The k-e model does a very poor job of predicting the hook pattern of the stern vortex. The q-w model does better, which is consistent with the results of Gorski and Coleman (2002) who showed the q-w model tended to be less dissipative than the k-e model for another vortical flow. However, the full Reynolds stress model most closely produces the hook shape of the vortex seen in the experimental data consistent with other results from Gothenburg 2000. It is difficult to form firm conclusions about what turbulence models are better. Simpler zero-, one-, and two-equation models do well for predicting much of the flow field, for many surface ships, particularly in regards to boundary layer development. They are also typically more robust and easy to use than full Reynolds stress models. However, if one needs details of a very complicated flow, such as a strong vortex, the higher order models may be necessary.

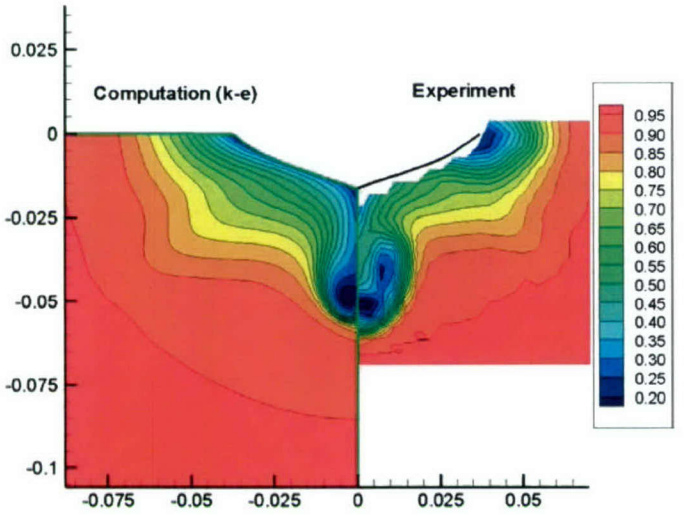

a)

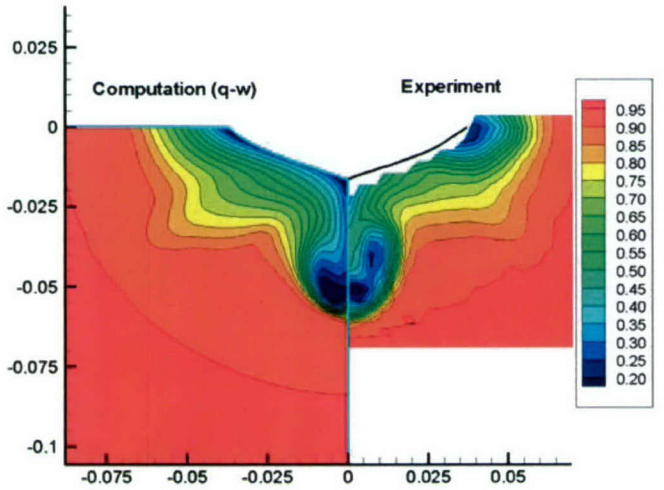

b)

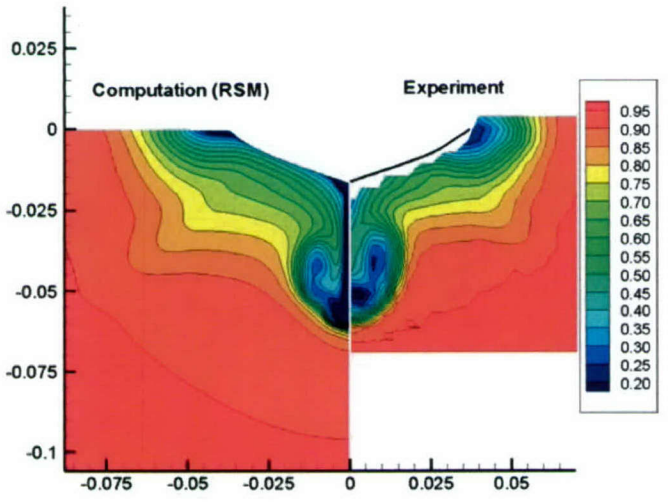

c)

Fig. 21 Comparison of computed and measured axial velocity: a) k-e model, b) q-w model and c) full Reynolds stress model.

MULTIHULLS

Although the previous examples have all been monohulls there is nothing preventing the application of RANS codes to multi-hulls. This is because there is typically no inherent assumptions about hull type in the RANS solver, particularly for the general purpose RANS solvers commonly used. It comes down to the ability to generate a grid on the geometry of interest and in that respect grids for multi-hulls are fundamentally no more difficult to generate than grids for monhulls. A few computations are shown here to demonstrate the capability.

SEA SHADOW

The Sea Shadow is a Small Waterplane Area Twin Hull (SWATH) developed to explore a variety of surface ship technologies, Scragg et al., (1998). The twin lower hulls are "Coke Bottle" shaped bodies of revolution designed to minimize wave drag at the design speed of 13 knots. These hulls are not parallel, but are canted with noses outboard and upward slightly. The struts are made up of flat planes which taper down to the intersection with the lower hulls. These struts are tangent with the lower hull on the outside, but the intersection is filleted on the inside. For the computations it is not necessary to include the upper body as we are only interested in the subsurface flow. However, it is necessary to grid the struts at least to the design waterline and consequently the intersection of the struts and lower hulls. There is also an appendage suite on each hull consisting of two control surfaces on the inboard sides and a propeller guard on the outboard side. A RANS computation for this flow with a linearized free surface approximation has been done and the computed wave height is shown in Fig. 22. Here the red contours indicate wave peaks and the blue wave troughs. The computations are at model scale, but at a Froude scale to correspond to the full scale ship operating at 13 knots. As can be seen there is much interaction between the two hulls both directly between them and in the formation of the rooster tail which forms downstream. The RANS computation is able to capture this interaction effect. The present computation was done for ½ the ship with port/starboard symmetry assumed, but it would also be possible to include the entire ship in a computation and allow for asymmetries between the port and starboard sides.

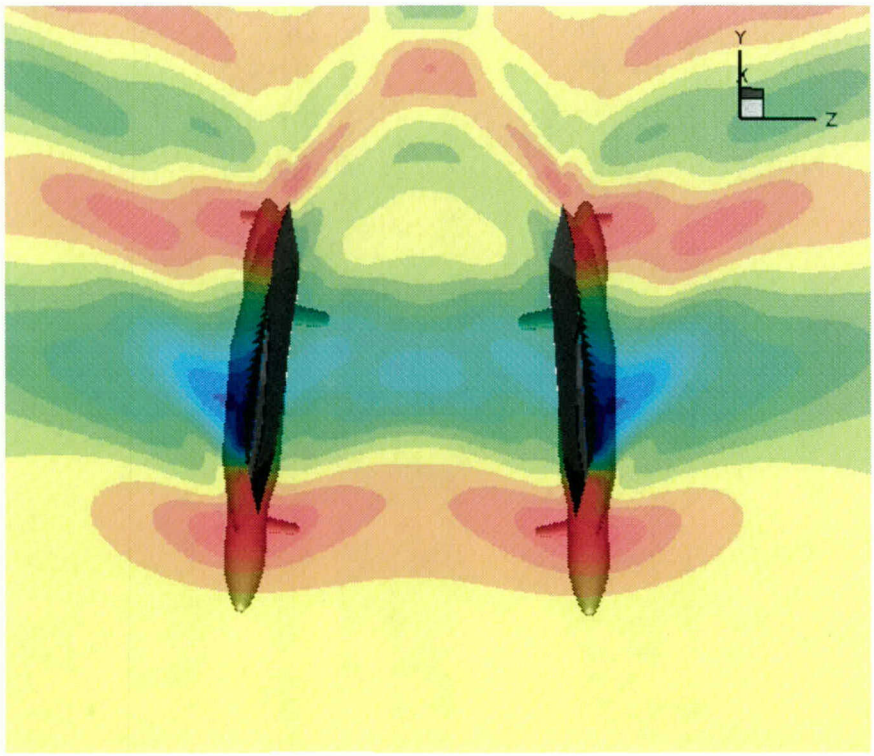

Fig. 22 Computed free surface heights for the Sea Shadow.

Shown in Fig. 23 are computed surface streamlines for the hull on both the inboard and outboard sides. Although the hulls are similar to axisymmetric bodies the flow is not straight down the length of the hull due to the angle of attack on the hulls, the coke bottle shapes, and the large struts. In addition, the necklace vortices forming around the inboard and outboard appendages is clearly shown as well as the impact of the angle of attack on these appendages. Despite all this it can be seen in Fig. 24 that the axial velocity develops along the hulls much as would be expected with and axisymmetric body and the changing radius of the hull has no apparent negative effect. The main deviations from a simple flow are created by the strut and appendages. Cross sections of the axial velocity at X/L = 0.68 and 0.85 are shown in Fig. 25. The forward plane indicates the wake of the inboard stern appendage is significant and there is much interaction between the main strut and the lower hull. At the further downstream location the inboard appendage wake persists, but there are also wake effects from the outboard propeller guard as well as the main strut. The different wakes can even be seen to interact to some extent since they have gotten so wide relative to the axisymmetric body radius. This all leads to a rather complicated non-axisymmetric flow field that enters the propeller.

Fig. 23 Computed surface streamlines on the lower hulls and struts.

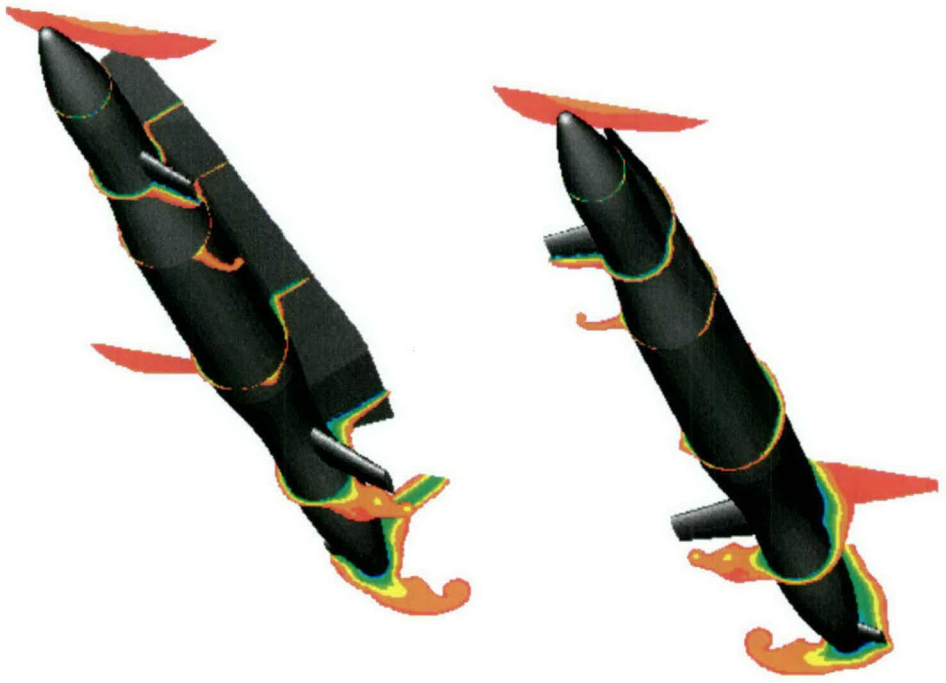

Fig. 24 Computed axial velocity contours along the hull.

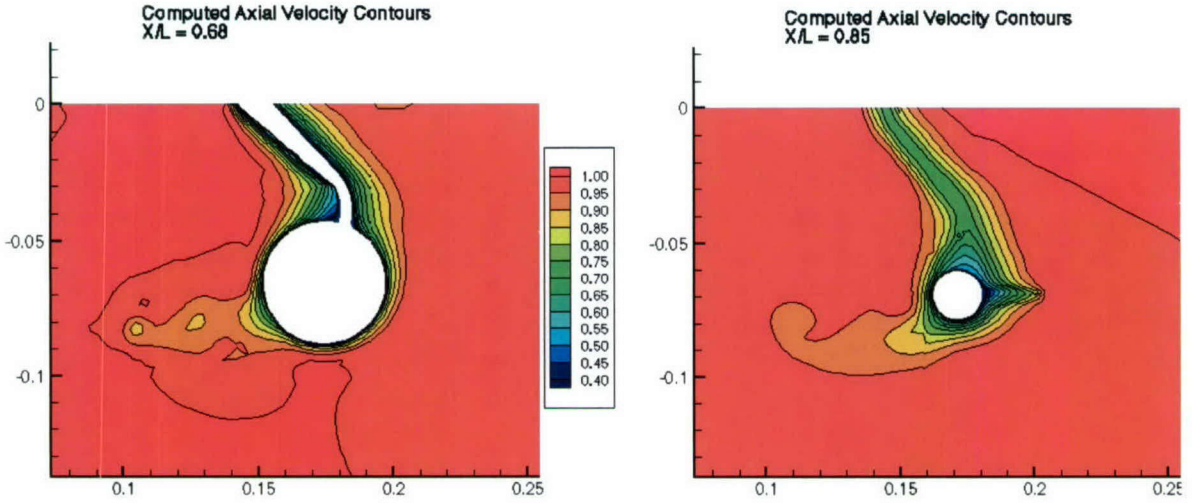

Fig. 25 Axial velocity contours at X/L =0.68 and 0.85.

TRIMARAN

As already mentioned, multihulls prove no more difficult to compute with RANS codes than monohulls. To demonstrate this a calculation for a notional trimaran is also performed. For many of the trimarans of interest for HSSL the main hull is often a long slender body with a slenderness much finer than conventional hulls. The flow fields for these hulls also tend to be somewhat benign as seen in Fig. 26, which has the computed surface pressure and streamlines for this notional hull. Flow generally flows down over the bow and runs smoothly along the length of the hull. This is similar to the *Athena* bare hull flow field computed by Ebert et al., (2003) and shown in the next section as fitted with twin waterjet propulsors. The hulls often have this flat stern section as waterjets are often under consideration to propel such ships and at high speed they can start to plane and become semi-planning hulls. For this example the streamlines on the outriggers are also seen to be rather benign.

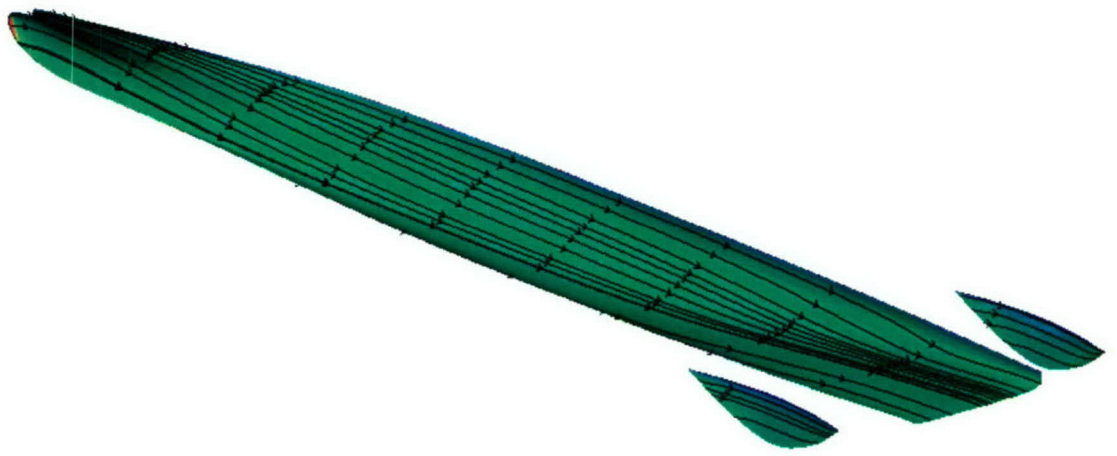

Fig. 26 Computed surface pressure and streamlines for a notional trimaran.

The axial velocity along the front of the hull is shown in Fig. 27. As might be expected from the streamlines there is basically a boundary layer formed along the length of the hull with no complicated interactions or vortices present. Because of the shape of the hull and the generally downward flow over the bow there is a thicker boundary layer on the keel than the sides of the hull. At the stern, Fig. 28, it can be seen that the flow along the keel has a much thicker boundary layer than to either side, which can impact waterjet performance. In addition, thin boundary layers form on the outriggers. However, this flow is much less complicated than the typical monohulls demonstrated previously. The main issues with trimarans is dealing with the free surface interactions and the potentially radical change in wetted surface area from slow speed, where much of the hull is submerged, to high speed where much of the hull may be out of the water. The propulsion system can also have a strong impact on the flow in the stern region and efforts are underway to include waterjet propulsion systems in RANS calculations as demonstrated in the next section.

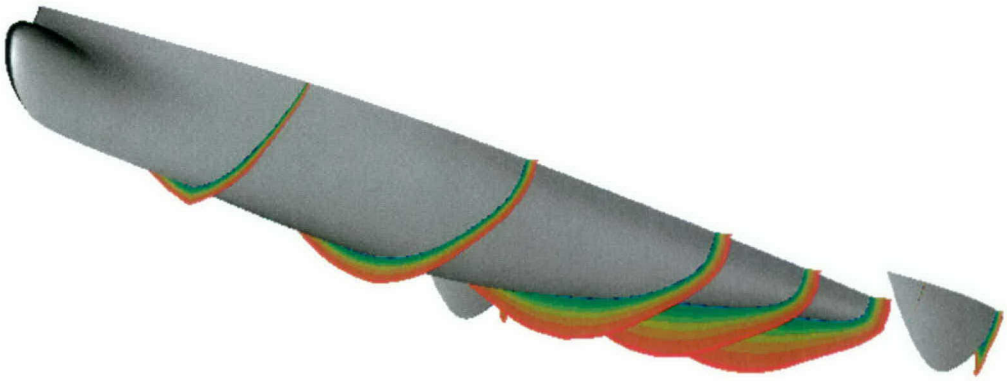

Fig. 27 Computed axial velocity over the front of the trimaran.

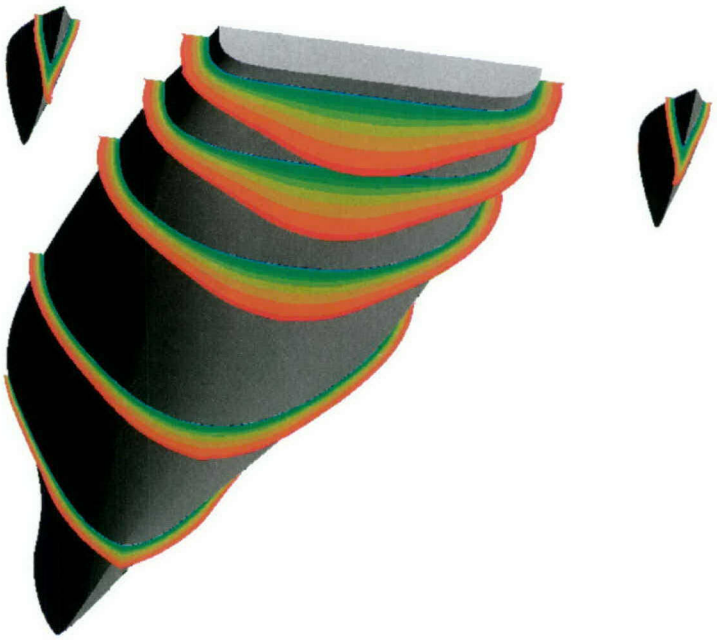

Fig. 28 Computed axial velocity over the stern of the trimaran.

WATERJETS

The desire for higher speed and necessity of operating more often in shallow-water environments for naval vehicles has motivated increased interest in waterjet propulsion systems. Waterjets have been identified as a viable means of propulsion in the higher speed regimes as conventional propellers could become problematic and experience severe cavitation and a related loss in efficiency. In addition, waterjets offer advantages for shallow draft operation and improved maneuverability. Consequently, waterjets are of interest both for smaller ships such as LCS as well as larger ships under consideration for HSSL. For HSSL designs in particular, high-power waterjets are deemed the propulson system needed to reach the required speeds (NSWCCD, 2002) and crucial to such designs is the integration of the hull and propulsor for better powering efficiency and reliable operation in sea conditions. Using RANS computations may provide an ideal means to study and evaluate the propulsor/hull interaction effects related to waterjets as well as the inflow that would directly impact efficiency. Consequently, efforts have been underway at NSWCCD to use RANS codes for computing waterjet flow fields.

ATHENA

One waterjet computational effort is described by Ebert et al., (2003), where computations are performed for a conventional hull that corresponds to the research vessel Athena, a former U.S. Navy PG 84 class ship. Dual flush, elliptical inlets were developed as part of a research program (Allison et al., 2001) where computations were undertaken to help evaluate and support the design of the waterjet propulsion system. Shown in Fig. 29 is the axial velocity through the inlet at various locations with the shaft present. The calculations are performed at a model scale speed of 8.55 knots, which corresponds to a speed of 25 knots at full scale. The Reynolds number based on ship length is 2.14×10^{7}. As can be seen in Fig. 30, which is the axial velocity at the pump inlet, the shaft creates a wake due to the upward component of velocity coming through the inlet. In practice, the shaft rotates and can have a significant effect on the pump inflow as shown in Fig. 31. Here it is shown that the rotating shaft tends to drag its wake around behind it creating a different propeller inflow than when the shaft is not rotating.

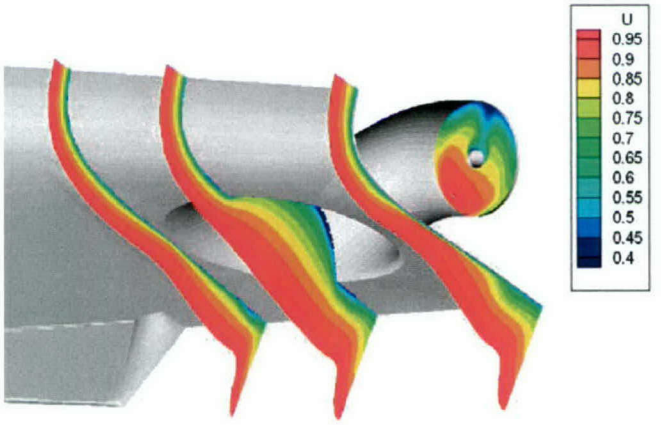

Fig. 29 Axial velocity contours through the inlet of the Athena with shaft included.

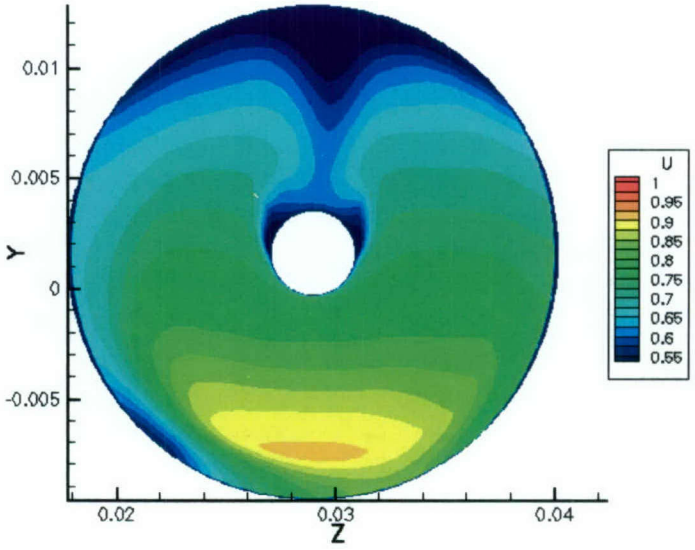

Fig. 30 Predicted axial velocity contours at the pump inlet with a non-rotating shaft.

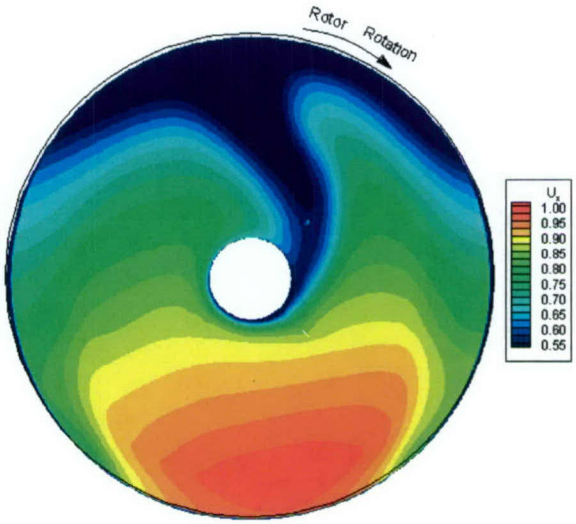

Fig. 31 Predicted axial velocity contours with a rotating shaft.

One thing to note with such RANS calculations is that the entire flow field is available for extracting details that may be of importance. The various examples have largely shown axial velocity, surface streamlines or pressures. However, it is possible to obtain more information than this such as streamlines in the flow field. This is of particular interest for waterjets where it is possible to use streamlines that enter the propulsor to accurately identify the capture area anywhere upstream of the inlet. This is demonstrated in Fig. 32 where streamlines entering the inlet are traced upstream to a plane on which an axial velocity contour is shown. More details of this computation can be found in Ebert et al., (2003).

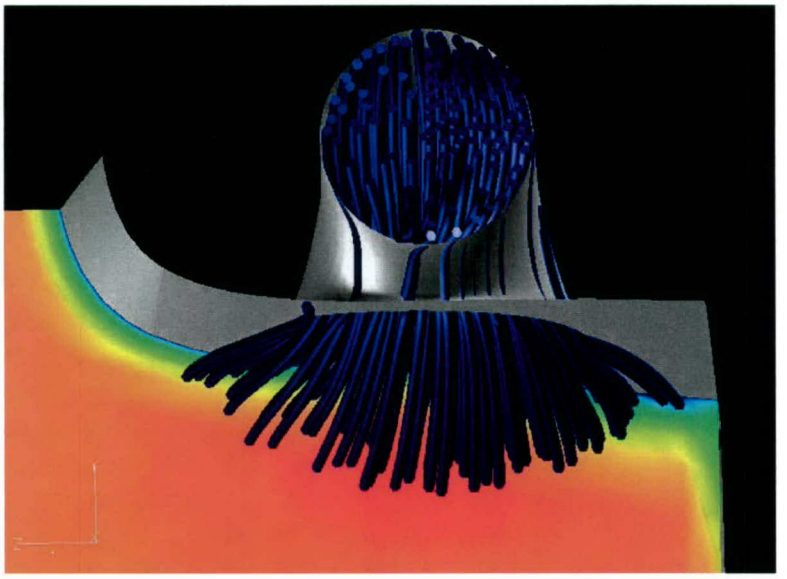

Fig. 32 Streamlines entering the inlet trace to an upstream plane.

AWJ-21

The second configuration is a notional future naval destroyer fitted with twin waterjet propulsion units faired into nacelles attached to the hull. The waterjets are fully submerged resulting in a below water discharge. The propulsion unit used is a Rolls-Royce Naval Marine Advanced Waterjet 21 (AWJ-21^{TM}). The pumps are driven by means of an inclined shaft that penetrates through the inlet ramp forward of the pump. A graphical depiction of this configuration with the hull, shown in red, and the waterjet nacelles, shown in green is in Fig. 33. The hull used in this case is a modified version of the hull studied as part of the ONR Accelerated Hydrodynamics S&T Initiative and shown previously in Fig. 15 and described by Gorski et al.,(2002) and includes a bow dome. The grid for this geometry near the waterjet pumps was shown previously in Fig. 5.

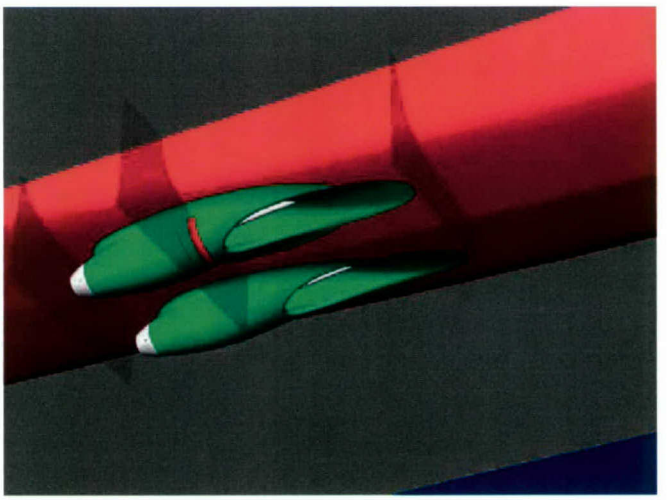

Fig. 33 Waterjet geometry for AWJ-21.

The computed configuration includes the hull, waterjet and rotating shaft with an actuator disk model used to simulate the pumping action of the waterjet. The thrust input parameter of the actuator disk model must be adjusted through an iterative process until the mass flow through the waterjet matches the experimentally measured mass flow rate. The calculations are performed for a model scale speed of 5.9 knots, which corresponds to a full scale speed of 28 knots. The Reynolds number based on ship length is 2.23×10^{7}. Since this is the same geometry as shown in Fig. 15 the flow field in front of the pumps is similar with the bow dome vortex being the dominant feature. These calculations are done with unstructured grids and it is possible to include the entire nacelle, both inside with the rotating shaft, and outside as part of the whole ship computation. A comparison of the RANS predicted axial velocity contours inside the pump upstream of the rotor with those measured experimentally, via LDV by Chesnakas (2001), are shown in Fig. 34. The LDV measurements are unable to collect data close to the shaft and walls of the inlet leaving blank regions adjacent to these surfaces. As also shown in the previous section with the Athena waterjet, the rotation of the shaft has an appreciable affect on the flow entering the pump. As can be seen the computation and experiment are in good agreement. It is also possible to obtain the inlet capture area as previously and other quantities needed to make performance predictions, based on the International Towing Tank Conference's "momentum flux method." More details of this and the computations in general can be found in Ebert et al., (2003).

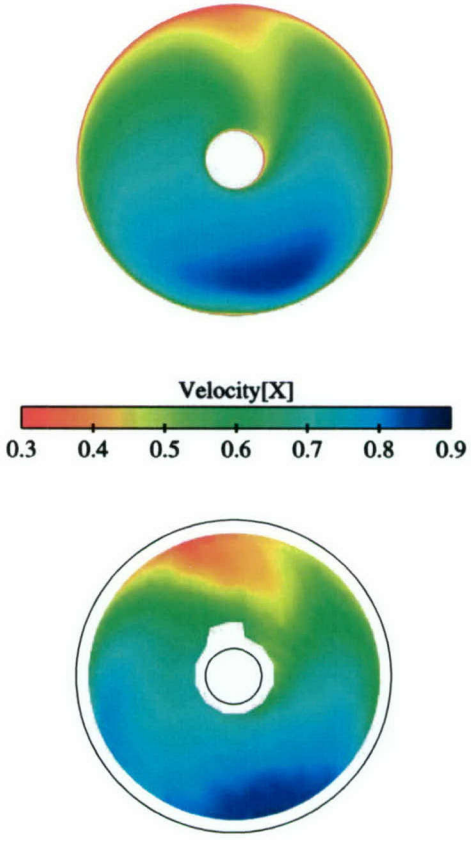

Fig. 34 Comparison of computed (top) and measured (bottom) axial velocities.

BILGE KEEL PLACEMENT

One of the key elements of economical and safe surface vessel operation is the proper alignment of appendages on the hull. By properly aligning appendages such as bilge keels, stabilizer fins, and support struts with the flow around the hull, total resistance, vibration, and acoustic signature can all be reduced. Consequently, appendage alignment has been a crucial component of model testing for the last hundred years. Inviscid calculation methods can provide some of the ideal flow over a ship hull and the effect of the free surface on it. However, due to requirements of roll stability and the necessity of operating in waves there are many possibilities for surface ship configurations. These configurations can lead to various vortices associated with surface ships that can be formed including bow, forward bilge and bow dome vortices (Gorski, 2001), which can potentially impact the streamlines around bilge keels. Consequently, inviscid methods cannot be used for appendage alignment. RANS however, does include such physics and as demonstrated by Krueger et al., (2002) RANS codes can provide an alternative to standard model testing for appendage alignment. By developing the hull streamlines computationally, surface appendages can be positioned on the hull with a high degree of accuracy relative to the incoming flow.

CG-47

An example of using RANS for bilge keel alignment is demonstrated here. A standard CG-47 hull was widened to increase its displacement. The hull is computed at a waterline of 7.132 meters (23.4 feet), which corresponds to a displacement of 10,860 tons. RANS calculations were performed on the bare CG-47 hull and the hull with a bilge keel in two positions. The calculations are performed at a model scale Reynolds number of 13.4 million and Froude number of 0.257, corresponding to a model scale velocity of 4 kts. Shown in Fig. 35 are the computed axial velocity contours at a number of constant longitudinal stations along the hull. The streamwise growth of the boundary layer on the hull and bilge keels is also shown, as is the growth of the bow bulb vortex and its interaction with the boundary layers. The RANS analysis of the appended hull streamlines show that the original bilge keel placement, based on the unmodified hull, is not properly aligned with the new flow. This is shown in Fig. 36 where a distinct gap is seen between the aft end of the bilge keel and the local streamlines, as well as the apparent turning of the streamlines around the trailing edge. A 3-dimensional CAD modeling program was used to realign the bilge keels to the modified flow in an attempt to smooth the flow over and behind the keels. The results are shown in Fig. 37, with the corrected bilge keel placement and the streamlines flowing more smoothly around the bilge keels. Kreuger et al., (2002) also demonstrate the placement of bilge keels on Model 5415. Although the above examples illustrate the potential for using RANS codes to help align the bilge keels it would also be applicable to other appendages such as the rudders and shaft struts.

Fig. 35 Computed axial velocity contours for the modified CG-47 hull.

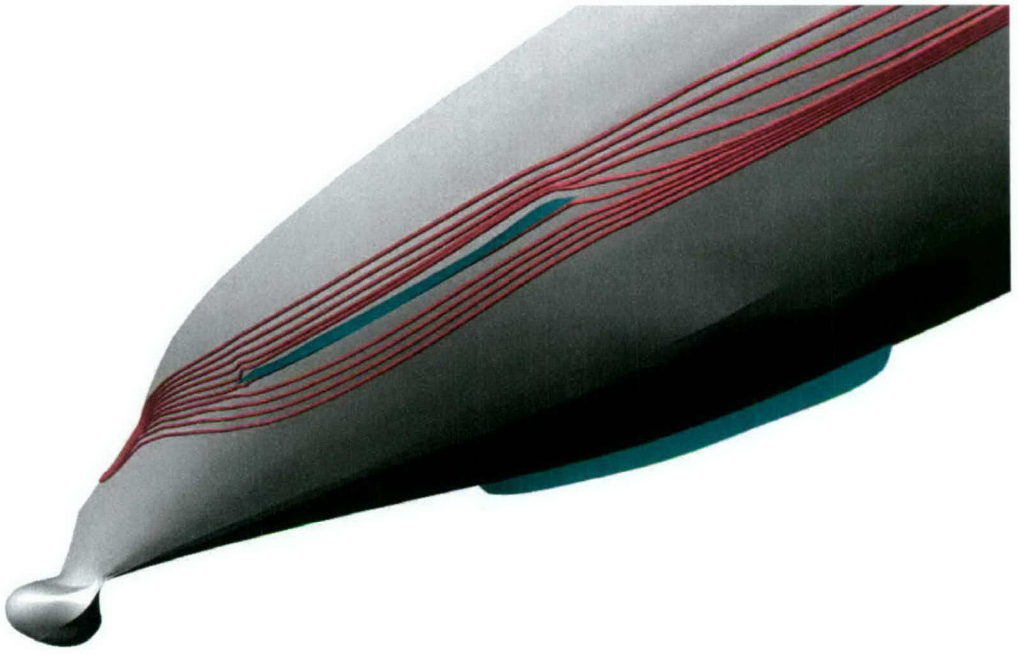

Fig. 36 Modified CG-47 hull, original bilge keel position.

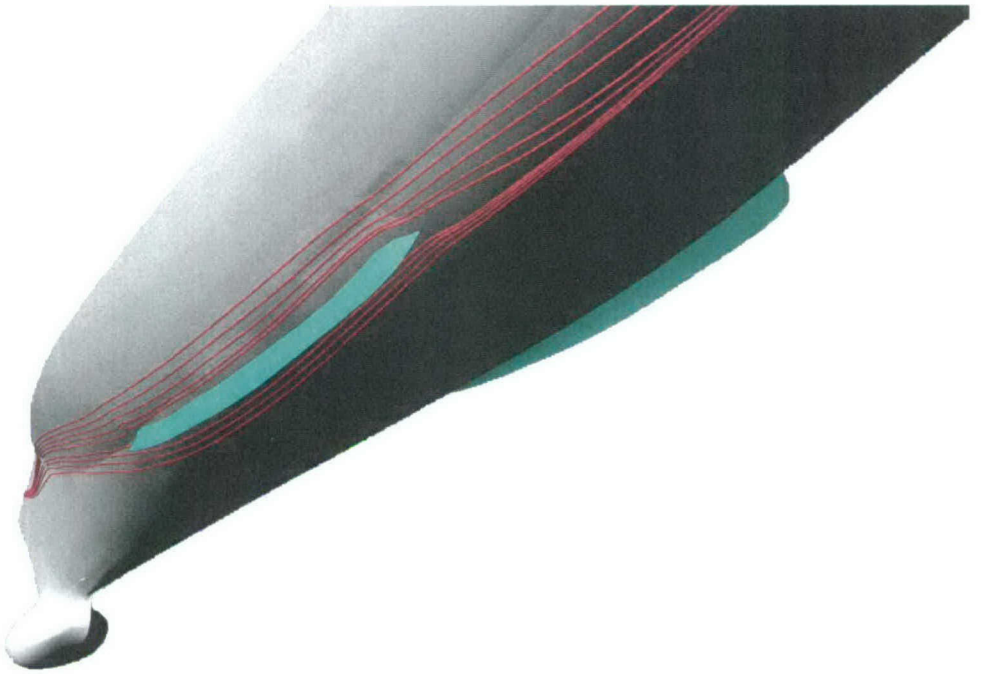

Fig. 37 Modified CG-47 hull, modified bilge keel position.

ROLL PREDICTION

Ship roll motion is another area where it is expected RANS codes can contribute. Roll motion limits ship operability, affects crew performance and ship habitability, and affects dynamic stability and ship capsize. Consequently, roll damping prediction is one of the critical but difficult parts of the motion prediction process. The roll motion of a ship is significantly influenced by viscous effects. Although the frictional roll damping on a hull form may not be significant, particularly at forward speeds, viscous related phenomena such as flow separation from the bilge and keels with the subsequent vortex formation account for a large amount of the roll damping. Bilge keels will significantly increase the damping of roll motions as well as generate a lift force if any forward motion of the ship is present. Predicting roll effects analytically has been problematic because of the significant viscous effects. Models for roll damping often include components related to frictional forces on the hull, lift forces generated on the hull and bilge keels and appendages as well as damping due to eddy generation of the hull and bilge keels (e.g. Himeno, 1981). However, when these models are applied outside of the data range for which they were obtained the results are suspect. Consequently, roll motion seems like an ideal area for RANS codes to contribute to seakeeping predictions.

An effort by Miller et al., (2002) demonstrates RANS simulations of roll motion for a 3-D cylinder, including bilge keels, with and without forward speeds. The calculations correspond to a 35.3-inch (0.897m) diameter cylinder with 2-inch (0.051m) wide bilge keels as tested in the Circulating Water Channel at the Naval Surface Warfare Center, Carderock Division. Measurements were made with the model fully and partially submerged. Forces were obtained over a 2-foot (0.61m) section of the bilge keels as roll motions were imposed at different frequencies and amplitudes. The vortices shedding from the bilge keels were also measured using a Particle Image Velocimetry (PIV) system attached to the rolling cylinder. Time

dependent RANS calculations were performed using about 3 million grid points on an IBM-SP3 using 84 processors. As seen in Fig. 38 due to the roll motion of the cylinder the bilge keel experiences an angle of attack and a vortex forms along the length of it. One must remember that this vortex is changing in time and will continually form on both the port and starboard sides as the hull rolls. The vortex formed on the previous cycle does not just disappear, but interacts with the new vortex that is formed. An example of the complexity of the flow that can be realized is shown with velocity vectors in Fig. 39. Here the flow field is at the point in time where the roll motion of the cylinder has reached its maximum and is just starting to go in the other direction. Consequently, we have a vortex that has formed on the lower side as the hull rotated counter-clockwise. The roll motion comes to a rest, but the vortex that formed still exists on the lower side of the bilge keel. Now, just as the cylinder comes to a complete stop and starts to roll clockwise a vortex starts to form on the upper side of the bilge keel with rapid flow around it. The RANS computation captures this effect very nicely as compared with the PIV data also shown.

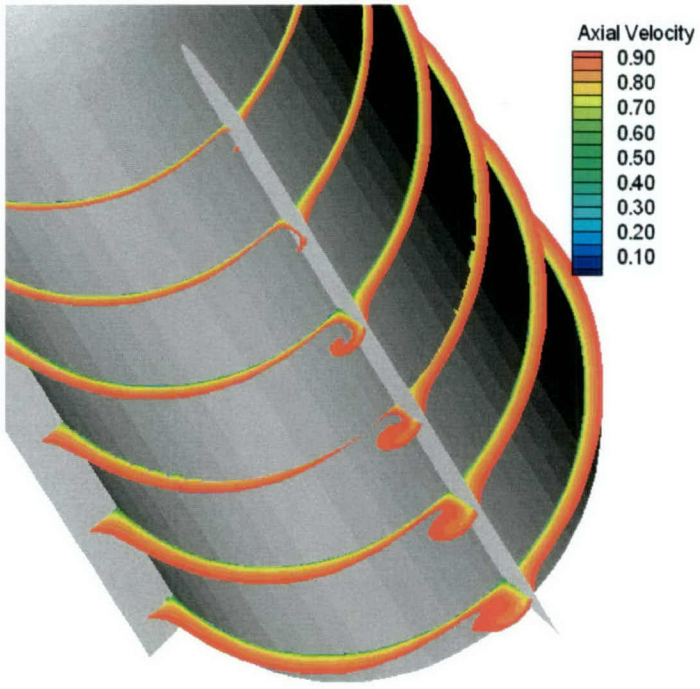

Fig. 38 Vortices formed along the bilge keel during a roll period.

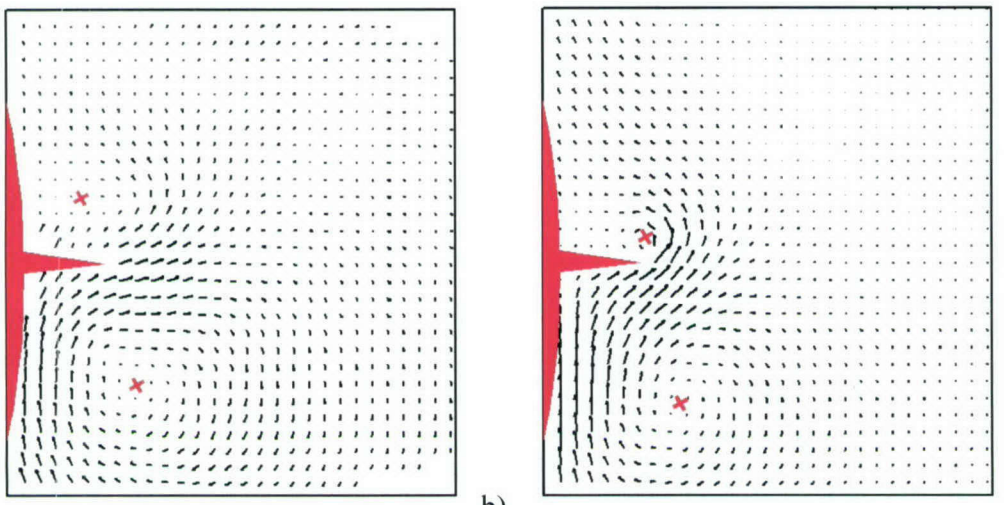

a) b)

Fig. 39 Computed and measured secondary velocity vectors at the end of a roll cycle; a) PIV, b) RANS computation.

A representative comparison of the calculated and measured force on the bilge keel for one period of roll motion is shown in Fig. 40. This is for a 15 degree amplitude roll with and without forward speed. The angular roll velocity at which the model is forced to roll is also shown in the figure. The figure shows that the RANS calculations accurately predict both the magnitude and phase of the measured data as well as the highly oscillating variations in the force data. The rapid acceleration and deceleration of the actual roll motion causes the sharp peaks in the force data. More comparisons with data and details of the calculations can be found in Miller et al. (2002). From these calculations RANS shows promise for predicting roll motions, but more evaluation needs to be done particularly for roll decay. Currently, computations are underway for Model 5415. With such RANS calculations it should be possible to also evaluate scale effects between model and full scale.

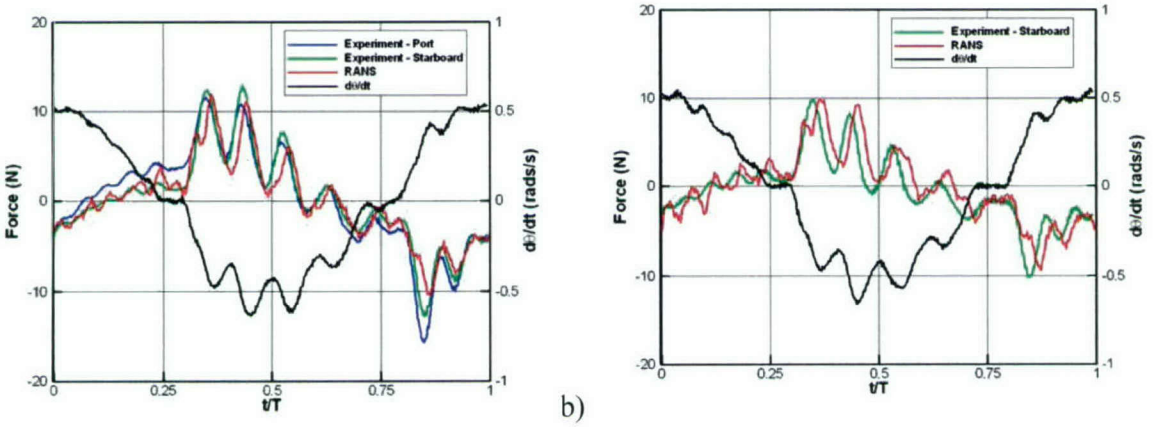

a) b)

Fig. 40 Forces for cylinder roll from Miller et al. (2002); a) zero forward speed, b) forward speed = 1.0 m/s (2kts).

MANEUVERING FORCES

Another area where RANS capability can contribute is in the prediction of maneuvering forces. In fact, the ITTC (1999) noted the considerable progress that had been made with RANS solvers and recommended that CFD approaches be pursued to reduce the number of experiments needed. Maneuvering predictions for surface ships typically refer to the horizontal plane forces. At any yaw angle vortices are shed from the underside of a ship much like tip vortices from a wing. To obtain the lateral forces the hull can be treated as a low aspect ratio lifting surface and estimated using slender body theory (Kaplan et al., 2002). However, the geometry of a surface ship is much more complicated than a wing and these methods must be supplemented with experimental data to properly model the forces generated by particular hull forms. Three-dimensional panel methods can be used to introduce much of the complexity of the hull, but they cannot provide the effect of the generated vortices. Because the forces generated by a ship hull are so dependent on the strength and position of these hull generated vortices, these methods must be supplemented with experimental data or a priori knowledge of the vortex field. RANS computations can provide these forces and flow information and a number of efforts are underway to better use RANS codes for maneuvering and seakeeping problems, some of which have been reviewed by Gorski (2002b).

YAW COMPUTATIONS

Computations have been performed for Model 5415 at various yaw angles from 0 through to 90 degrees. As mentioned these flow fields can be very complicated due to the vortical flow structure created. To demonstrate this flow complexity, shown in Fig. 41 is the computed axial velocity contours at a 20 degree yaw angle computed at model scale. The dominant feature is the vortical flow generated from the keel line just behind the bow dome, which has many similarities to a tip vortex shed from an appendage. Complicating the flow field is the bow dome creating its own wake structure and a second vortex is formed near the stern from the skeg. Additionally, just downstream of the formation of the primary vortex there are interactions of the flow near the keel line as well as the vortex "pulling" boundary layer flow off of the hull. At different angles of attack these interactions change, but RANS calculations should be able to predict them. At very high angles of attack the flow gets more complicated with large separated regions. These large angles of attack should be of interest for estimating cross flow drag. For the beam case, Fig. 42, the flow is highly complex with distinct differences between the bow, stern and midship regions. The flow near midships appears to be two-dimensional and similar to the flow passing over a blunt body with separation behind it. At the bow and stern the flow separates from the keel line and there are more three-dimensional effects, probably due to the flow coming around from the sides. For a bare hull such as this, a variety of yaw angles can be computed quite readily with a double body approximation providing force and moment data. The predicted lateral forces versus yaw angle for this hull form are shown in Fig. 43, which contains both the total side force and that component of the lateral force due to shear stresses at model scale. The viscous shear stress force on the hull is small, compared to the total force, so the dominant component is from the pressure differences on the hull. This does not mean that viscous effects are unimportant. The vortical structure generated from the hull has a large effect on the surface pressures. This is demonstrated further in the discussion on scale effects.

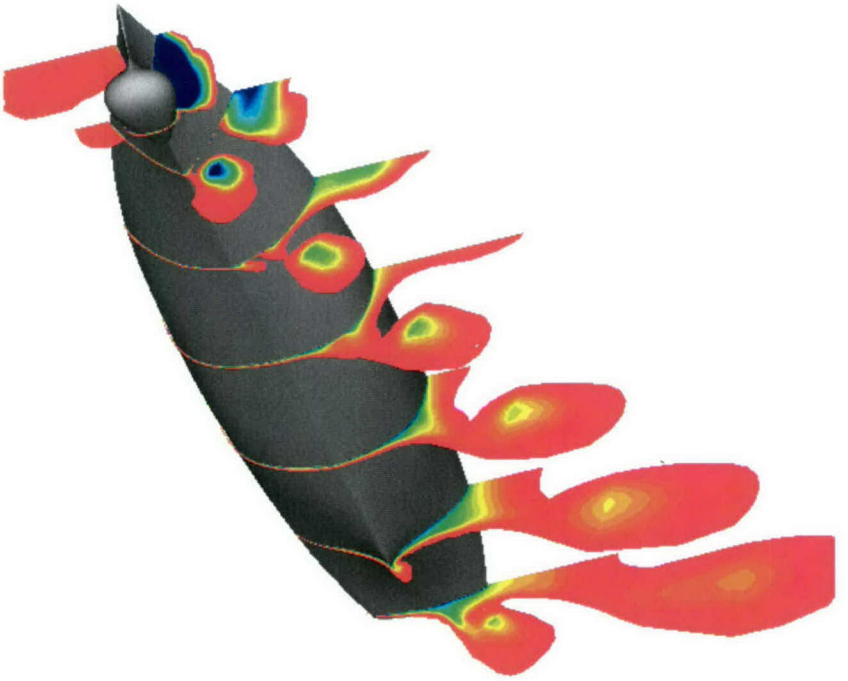

Fig. 41 Axial velocity contours for 20 degree yaw case.

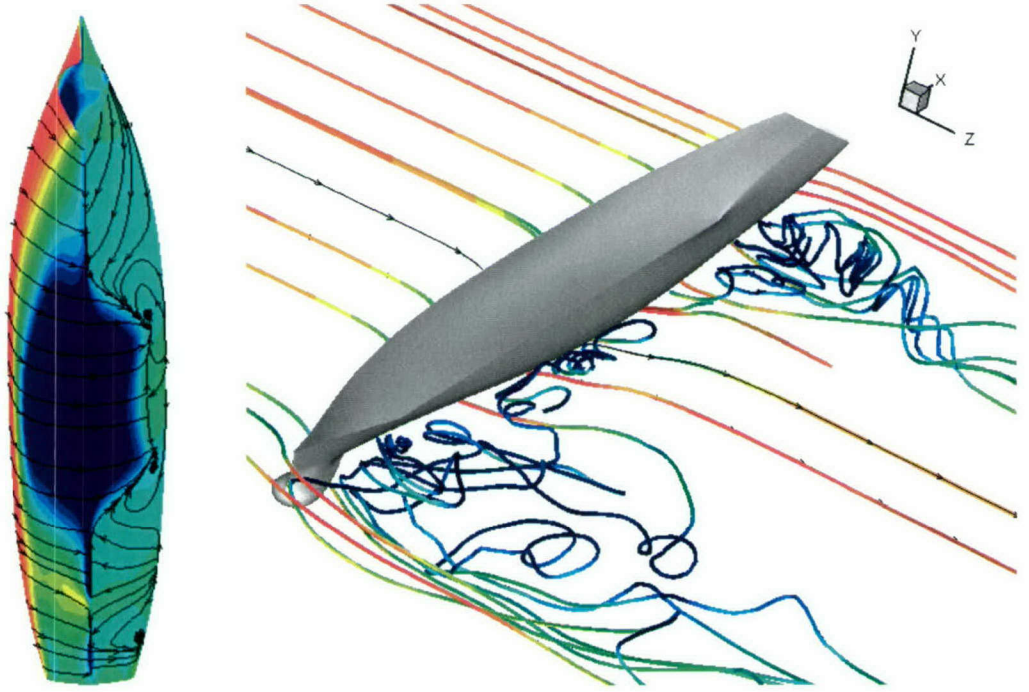

Fig. 42 Computed flow field for beam flow.

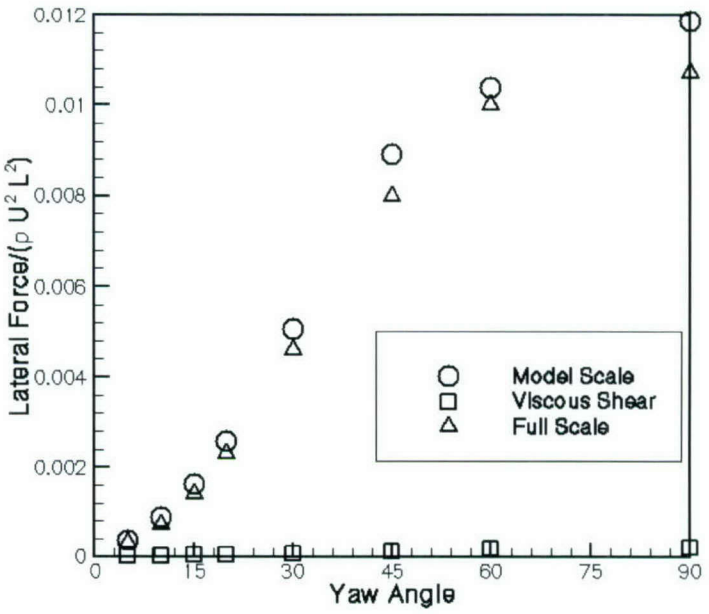

Fig. 43 Computed lateral forces.

STEADY TURN

The above computations demonstrate the flow fields for various yaw angles. It is also straightforward to obtain similar information for a turning ship and results have been demonstrated for a variety of turning hull forms in the literature. Unlike a constant yaw angle, where the entire ship experiences the same angle of attack, a ship undergoing a turning maneuver will experience different angles of attack along the length of the hull. This is demonstrated in Fig. 44 for DTMB Model 5415. For this orientation, and turning diameter of six ship lengths, the flow over the bow is from port to starboard and creates a wake on the starboard side near the bow. Again a vortex is formed from the keel similar to what was shown previously. The hull rotates about its midships section so the port to starboard flow is a maximum at the bow, decreases to zero at midships, and becomes a starboard to port flow at the stern. Consequently, past midships the starboard to port flow starts to dominate and the keel vortex that formed is pushed from the starboard to the port side and a new vortex starts to form along the keel at the stern. These calculations can be run as steady predictions and obtained similarly to the yaw cases already shown to obtain force information for various hulls. RANS calculations provide the entire flow field, make it possible to visualise what is occurring physically, and may help researchers understand the flow. This could also lead to better modeling of particular aspects of the flow field.

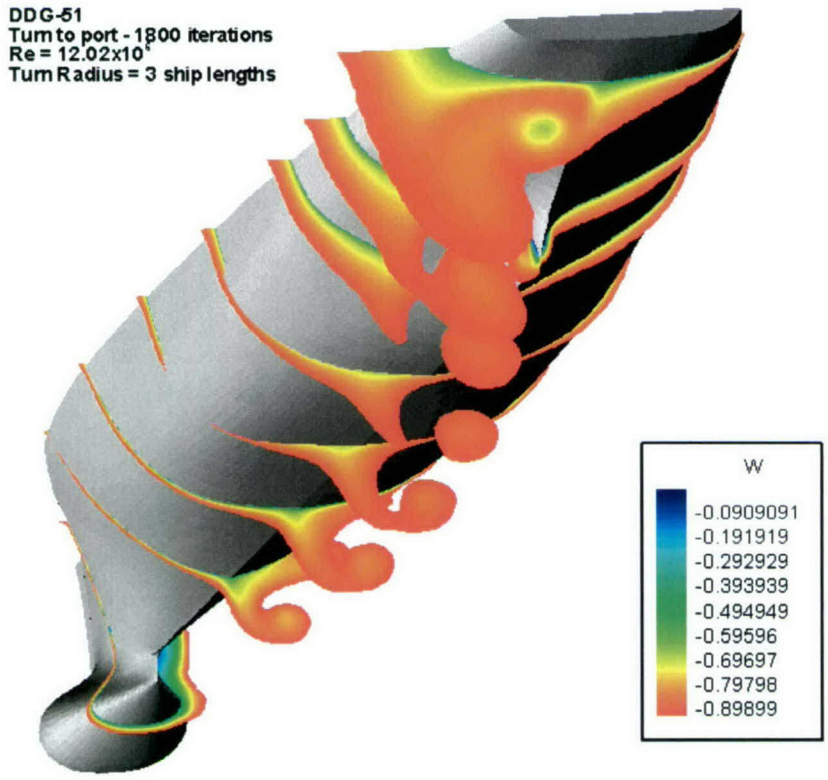

Fig. 44 Axial velocity contours for Model 5415 in a turn.

FULL-SCALE EFFECTS

RANS calculations for predicting full-scale ship flows are becoming more routine. However, there are issues involved in the full scale calculations in addition to the need for more grid points for boundary layer resolution. Models tested are often smooth allowing surface roughness to be ignored. Real ships are considerably rougher as built and only worsen with time at sea. However, surface roughness is often ignored, Patel (1998), as in the current full scale simulations. Hence, the full scale computations probably predict thinner boundary layers than actually exist and care must be taken when interpreting the results. However, there are definitely boundary layer changes between model and full scale. RANS provides an opportunity to look at the potential ramifications of this change in boundary layer thickness. The main differences are in propeller inflow, but changes can also be seen in the maneuvering forces due to boundary layer effects. There is also a potential for some differences in the wave field as also shown.

PROPELLER INFLOW

Propeller inflow is probably most impacted from model to full scale. This will be particularly true for integrated proupulsor/hulls and waterjets where the propulsor is operating in the boundary layer. Even for conventional hull configurations the differences can be significant where the model scale boat has the propeller inflow heavily influenced by the hull boundary layer, but the much thinner boundary layers of the full scale ship allow the propeller to operate outside of the boundary layer. This is demonstrated here for a destroyer with further details in Gorski et al., (2004). The model scale computations for DTMB Model 5415 both appended and

unappended was already shown. For full scale conditions the Reynolds number, based on length, is approximately two orders of magnitude larger than the model scale Reynolds numbers and the Froude number is kept the same. For the bare hull calculation the flow field itself is very similar to the model scale flow, shown in Fig. 6, but with a thinner boundary layer and smaller vortex structure formed over the front of the hull. This leads to a thinner wake at the propeller plane as shown in Fig. 45. Here a comparison with the model scale predictions indicates that there is almost no hull wake entering the propeller disk, indicated by the circle, at full scale compared to what would enter the disk at model scale.

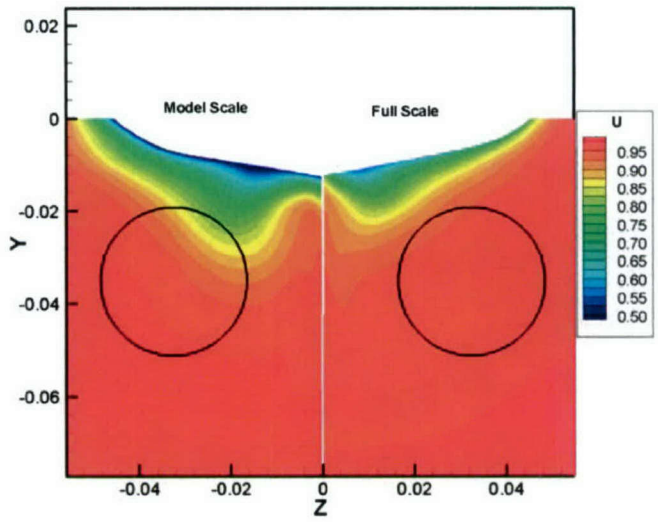

Fig. 45 Bare hull model and full scale prediction at the propeller plane.

The full-scale calculation performed for the shafts-and-struts configuration also exhibits significant differences from the model scale predictions in the flow at the propeller plane. Here the Reynolds number is set to 1.4 billion, based on length. Results for this calculation are shown in

Fig. 46. The shaft wake is still evident as are the wakes of the struts. However, it is seen that the size of these wakes is reduced significantly, as compared to the model scale computation shown previously in Fig. 7. Additionally, the hull boundary layer and vortex structure is reduced significantly. Consequently, only a small portion of the propeller disk experiences a flow disturbance as almost none of the flow from the hull boundary layer/wake enters it. This is consistent with the bare hull calculation of Fig. 45. However, the shaft and strut wakes are still present and are the only significant deviation from the free stream flow entering the propeller disk, Fig. 47. A comparison of the averaged axial velocity through the propeller disk area demonstrates the significance of this. The axial velocities for model and full scale entering the propeller disk are shown in Fig. 48 and then integrated to provide and average axial velocity. Both of these computations contain the shafts-and-struts. The results for the model scale indicate the average axial velocity entering the propeller is 0.939 of the free stream velocity. The full-scale results for the shafts-and-struts configuration, where the wakes provide less velocity deficit than the model scale case, raises the average velocity to Uave = 0.972. Consequently, care must be exercised when using model scale experimental data to infer full scale propeller inflow.

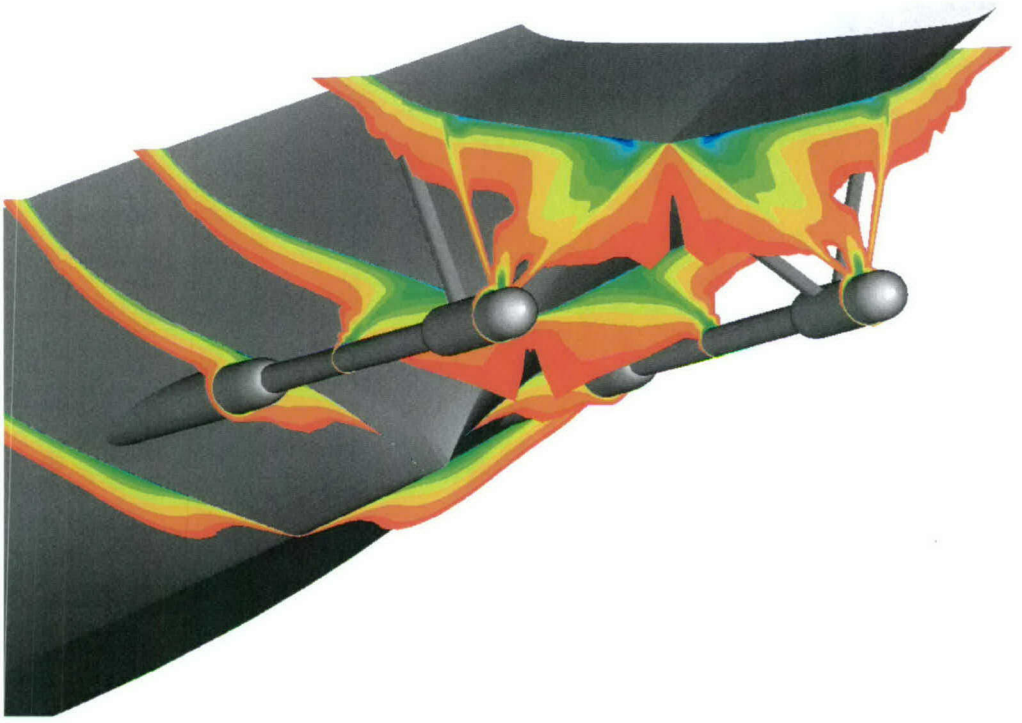

Fig. 46 Computed axial velocity contours at full scale.

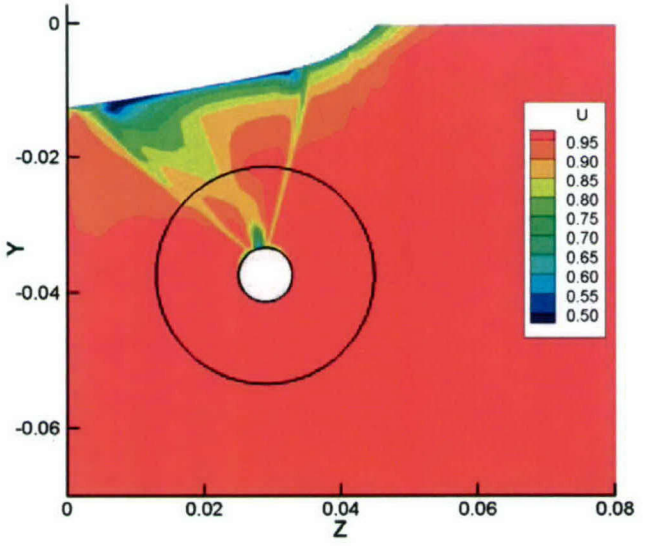

Fig. 47 Computed axial velocity at the propeller plane at full scale.

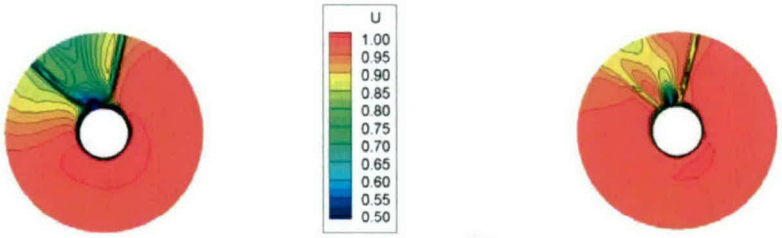

a) b)

Fig. 48 Comparison of flow at the propeller disk and average axial velocity: a) Model scale, Uave = 0.939, b) Full scale Uave = 0.972.

WAVE HEIGHT

To get the propeller inflow to a surface ship viscous computational methods such as RANS codes are needed. RANS type codes are not generally needed for predicting the wave field as invisicid methods have worked very well for predicting wave heights and wave drag in general. This is because viscosity does not have a dominant impact on the wave generation and propagation near the hull. Similarly, if the wave field does not have a strong impact on the propeller inflow double body approximations with RANS codes can be used very effectively for predicting the propeller inflow. However, RANS codes do need to have a free surface capability as there are many cases where the interaction of the free surface and the boundary layer flow are important and influence each other. A verification of the role of viscosity, or lack thereof, in the free surface wave field of Model 5415 is now shown. As already discussed for Model 5415 the dominant flow feature for this hull is a vortex created at the sonar dome that flows downstream to the propeller plane. As just shown, Fig. 45, the full scale the boundary layer will be thinner and the computed vortex location will be relatively closer to the hull. However, this difference in boundary layer has negligible impact on the computed free surface heights. This can be seen in Fig. 49 where computed free-surface contours at Fr = 0.2758 for Model 5415 at model and full scale Reynolds numbers are shown. The top portion of the figure is a model-scale calculation, while the bottom portion is full-scale. As can be seen the Kelvin waves along the hull appear very similar for these cases which is expected as the viscous boundary layer and vortices should have little impact on them. However, there is definitely an impact behind the stern as seen in Fig. 50. Here it is seen that the higher Reynolds number, with its relatively thinner boundary layer, leads to a rooster tail that is both higher and farther downstream than the model scale calculation. It is not unexpected that differences in the wave heights would show up in the transom and stern regions as this is where the differences in boundary layer thickness will be most evident. It is also expected that such differences in flow behavior at the stern could lead to differences in the amount of transom which is wet or dry and subsequently impact overall resistance in more ways than just ITTC friction line differences and really be impacting form drag with Reynolds number.

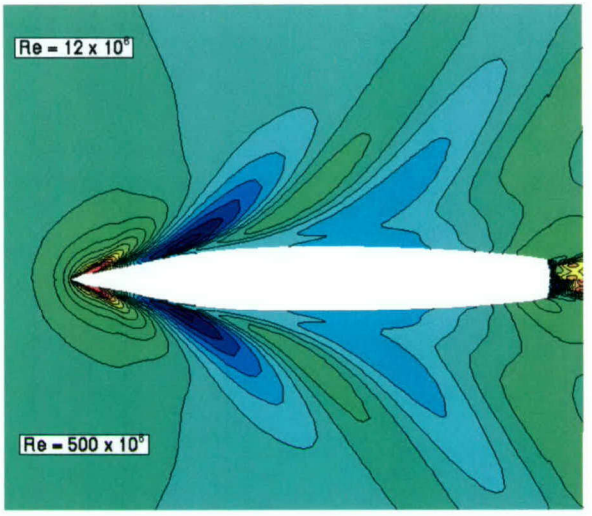

Fig. 49 Computed free surface height for Model 5415 at model and full scale.

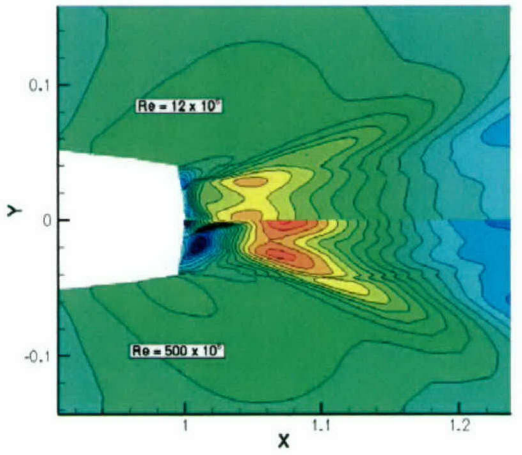

Fig. 50 Computed free surface heights in the stern of Model 5415.

MANEUVERING FORCES

The differences in boundary layer flow between model and full scale also impact the maneuvering forces. Although the viscous forces themselves are small compared to the pressure forces the vortical structure generated from the hull has a large effect on the surface pressures. At full scale the boundary layers are relatively thinner and the resulting vortical flow structure is also affected. A comparison of the computed axial velocity at X/L = 0.895 at both model and full scale, Reynolds numbers of 12 and 900 million based on body length, for the Model 5415 destroyer are shown in Fig. 51 for a 20 degree yaw angle. Although the flow is similar, the different hull wakes and vortex strengths lead to differing flow fields on the hull. This can be seen in Fig. 52, which has surface streamlines and pressures for these two calculations. The limiting streamlines created by the hull generated vortex as well as the surface pressure has changed near the stern. These changes provide the force differences demonstrated in Fig. 43 between model and full scale. The differences seen for the lateral force are larger than the viscous shear force at model scale indicating the change of the overall flow field and its

resulting impact on the pressure field is probably a larger driver in scale effects than the viscous shear alone.

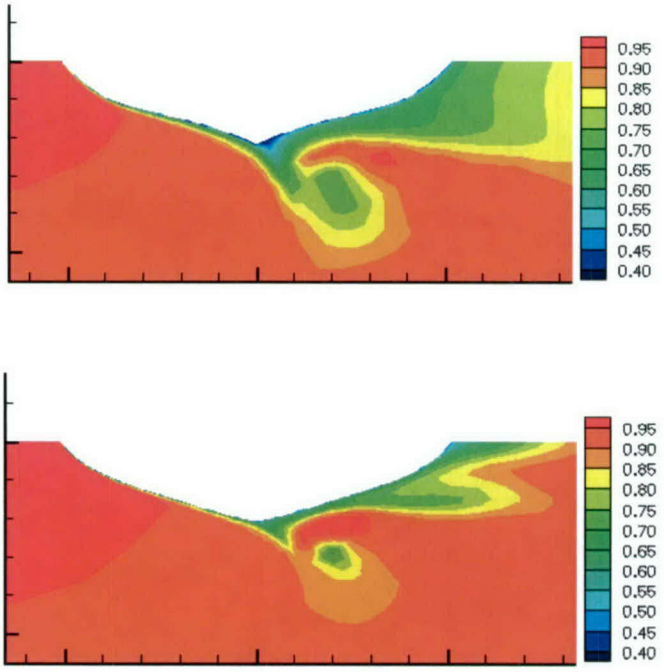

Fig. 51 Computed axial velocity contours at X/L = 0.895: a) model scale, b) full scale.

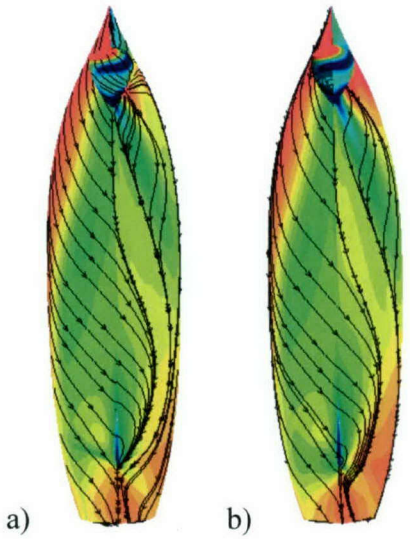

Fig. 52 Surface pressure and streamlines for 20 degree yaw case; a) model scale, b) full scale.

RANS/CFD PLAN FOR THE FUTURE

As demonstrated in this report RANS computational techniques are already able to provide many details of complicated flow physics of interest to the marine community. The computations can also provide guidance and insight on scale effects and are generally applicable to many configurations for which there is little or no experimental data. While RANS and CFD in general has yet to match early, extraordinarily high expectations, which started with talk of replacing conventional wind tunnels with "Numerical Wind Tunnels," its abilities and accuracy have improved steadily with increasing computer power and should continue to do so. It is not unreasonable to expect Moore's law, which predicts that computer power will double every 18 months, to continue for approximately the next 25 years.

Increased use of CFD is one way the Navy can capitalize on these computer advances and on DoD investments in programs like the High Performance Computer Modernization Program (HPCMP). Because computer architectures are changing so significantly, however, the Navy must realize that the software will also continue to change. To be used effectively, CFD needs a dynamic and changing environment that makes the best use of the advancing capability. A code that is "validated" today may be useless in the future. A good example of this is how many software packages changed from vector based algorithms to parallel based algorithms as parallel architectures matured. Additionally, CFD, which is often synonymous with RANS codes today, can and should encompass an entire suite of evolving codes from simple inviscid theory through Large Eddy Simulations (LES) and conceivably Direct Numerical Simulations (DNS) eventually. Often, to fully utilize current computational power it is necessary to start developing the computational tools 5 or more years before they are fully available. A strategy to most effectively use CFD encompasses three areas of focus: institutionalization of CFD, systematic validation, and design related studies.

The institutionalization of CFD does not mean replacing experiments with CFD, but developing the mindset of using CFD to accomplish some of what we currently do with experiments. Other organizations, like the DOE, that cannot do as much testing as the U. S. Navy have already had to develop this mindset. For example, the end of the Cold War brought a ban on nuclear weapons testing. Consequently, the nuclear weapons laboratories have replaced nuclear weapons tests with computational simulations. These simulations must accurately predict how each part of the weapon will behave during the detonation. As another example, the aerospace industry uses CFD with increasing frequency to predict flow over aircraft structures at flow conditions that cannot be replicated in the wind tunnel. In addition, as more aging wind tunnels in the United States are being shut down (and not being replaced), the aerospace industry is finding ways to use CFD to offset the loss of these test facilities.

Before 1874, ship performance was largely based on full-scale experience. It was then that Froude(1874) had the insight to split ship resistance into wave making and frictional components and to treat these components independently. With Froude's approach model scale data could be used to provide information on full-scale ships and there has been a tremendous amount of model scale experimental testing done to support ship hydrodynamics design and understanding ever since. Over a century of effort has gone into developing better experiments and into developing the infrastructure and experienced personnel to perform these experiments. The Naval Surface Warfare Center's Carderock Division alone has over $1.4 billion worth of hydrodynamics facilities. Organizations such as the International Towing Tank Conference (ITTC), established in 1932, have been set up to: "*stimulate progress in solving the technical*

problems that are of importance to towing tank Directors and Superintendents who are regularly responsible for giving advice and information regarding full-scale performance to designers, builders and operators of ships and marine installations based on the results of physical and numerical modeling." Despite all these efforts we still have significant issues with model scale tests. These problems include: how and where to "trip" models, facility biases, blockage effects, an inability to do tests for extreme conditions. We also require approximations like the ITTC friction line and correlation allowances for scaling to full-scale. The mindset, however, has been to develop ways to work around these shortcomings to most effectively use the model test data to elicit information for full-scale performance.

RANS, on the other hand, is relatively new. It was only a little more than a decade ago that the first RANS calculations were performed on a fully appended submarine, Gorski et al., (1990). By today's standards, the results had a poor resolution. It is even less than a decade ago that the ITTC(1996) concluded that RANS had matured enough to be integrated into the design process for issues associated with resistance and propulsion. Even more recently the ITTC (1999) recommended that CFD approaches be pursued to reduce the number of experiments needed for the prediction of maneuvering forces. On top of this there continues to be much success in RANS prediction capability and these trends will continue.

A way to start institutionalizing CFD is to go through design/evaluation processes computationally in parallel with the existing experimental-based approach, replacing experiments with computations where appropriate. Differences in the final product would need to be evaluated and possibly typical corrections for the experiments replaced with corresponding corrections for the computations. This would provide a way to determine the current state-of-the-art for computations as well as continued improvements in this process as computational capability improves.

Of course we need to predict model scale experiments accurately. Consequently, an effort must be established to continually perform systematic validation related studies to identify shortcomings in computational capability and to evaluate new software as it becomes available. To develop confidence in the capability, we must first demonstrate the tools on existing hull configurations where data exists. The tools must be able to handle a wide variety of geometry changes and subtle effects. We should perform a significant number of computations and address computational dependencies including: grid resolution, turbulence modeling, adaptive gridding, time dependent RANS, propulsor modeling, and uncertainty analysis. A significant experimental effort may be required to provide the necessary data for code and process validation. Many historic data sets are not reliable for CFD validation because of the poor data quality or insufficient documentation of the actual experimental conditions. Efforts in recent years have often attempted to acquire higher quality data specifically for CFD validation. There have also been efforts to "model-the-model" so we can truly evaluate differences in computations and experiments. Unfortunately, the level of CFD validation today often encompasses only a few single point calculations rather than systematic evaluation of the ability to predict the measured flow physics and increasingly complicated geometry variants. Ultimately, the CFD community needs to move toward providing predictions, with some level of uncertainty analysis, that can be trusted without the corresponding experimental data to back up the predictions.

Finally, if calculations are only done for a final design to replace a few tests, CFD is probably not cost effective. To be used effectively, CFD, much like experimental testing,

requires its own computer infrastructure and expertise. It will continue to be this way in the near future. The real benefit from CFD should come through design studies and eventually optimization techniques. Series tests used to be a way to develop a large database of knowledge to understand what design variations meant to performance. Series tests are rarely done today because of their expense. Often only a few tests are done on a final, or near final, design, and these designs are built based largely on experience developed in the past. This is a shortcoming in the current design strategy, which doesn't always make the best use of all of our available tools. CFD is an ideal way to perform series type tests. Computations played an important role in developing good designs for the Advanced Sail, Gorski and Coleman (2002). Numerous options were evaluated based on computations, and only the final designs for these programs were tested in the LCC. Because of cost constraints all the various options considered could not be tested. By using computations to eliminate less desirable options, we were able to test the most potentially successful geometries and provide significant risk reduction. CFD can also play an important role in design efforts by providing information on the flow field not available through an experiment. A recent example from the aerospace industry involves an abrupt wing stall during initial flight tests of the F-18E/F. This stall condition was not detected during wind tunnel testing, and numerous "fixes" subsequently evaluated in the wind tunnel failed to alleviate the problem in flight. The in-flight stall problem was finally duplicated with CFD simulations, allowing ultimate resolution of the problem. While detractors cite issues with the level of accuracy of computations, there will always be issues with both computations and experiments. Nonetheless, the computations can generally provide the correct trends, and this insight can help to improve design and testing. Optimization techniques, which are also evolving due to increased computer power, provide even more potential to lead to designs with enhanced capability that would not have even been considered with traditional approaches.

CONCLUSIONS

RANS codes are starting to play a larger role in the study of viscous flow fields generated by marine vehicles of naval interest. With increased accuracy and robustness, due in part to the advent of parallel computer capabilities and increased experience, it has been possible to move such computations to the point where they can impact design studies. Although this has largely been done for steady studies of resistance and propulsor inflow it is also progressing to dynamic areas for maneuvering and seakeeping. It seems inevitable that RANS will have an even larger role in the future as computer power increases and the application of such codes matures even further. RANS predictions can be a time and cost effective way to improve prediction capability for new designs where experimental data bases do not exist. However, it will still take considerable effort to have the confidence in the RANS codes that currently exists with the model tests.

RANS, and CFD in general, are not panaceas that can predict everything in a timely manner. They are tools that provide similar and different information than model tests. They require modeling and consequently have shortcomings just like experiments, but the foreseeable increase in computer power is very attractive from a time and cost perspective. To institutionalize CFD and develop more confidence in its capability is going to take effort. Fortunately, it should not take as long to evolve as model testing capability and is already having considerable impact for various problems. Of significance, and why CFD looks more promising now than it did a decade ago, is the maturing of parallel computation. This has added tremendous capability and may very well have allowed us to cross a threshold in applying

advanced computational techniques more quickly and accurately. CFD will continue to improve with advances in physics based modeling, meshing algorithms, and computer architecture. What was not imaginable for CFD ten years ago is routine today. By extension, much of what is not considered feasible for CFD today will likely be routine in ten years. The Navy would be ill-advised to underestimate the importance of CFD in the coming years.

REFERENCES

Allison, J. L., et al., "Research in Waterjet Inlet, Hull,and Jet Interactions," *Proc. Int. Conf. Waterjet Propulsion III*, Gothenburg, Sweden, Feb., 2001.

Beck, R. F. and Reed, A. M., "Modern Computational Methods for Ships in a Seaway," *Proc. 23rd Symp. Naval Hydro.*, Val de Reuil, France, 2000.

Chesnakas, C., Model 5415, DTMB Web page, http://conan.dt.navy.mil/5415.

Chesnakas, C. J., "3-D LDV Mapping of the Flow About a Waterjet-Powered Hull in a Tow Tank," *Proc. 26th American Towing Tank Conference*, Webb Institute, Glen Cove, New York, 23-24 July, 2001.

Clark, D. J., Ellsworth, W. M., and Meyer, J. R., "The Quest for Speed at Sea," Naval Surface Warfare Center, Carderock Division, Technical Digest, pp. 3-27, April, 2004.

Dailey, H. L., Ebert, M. P. and Miller, R. W., "Comparison of Unstructured and Structured RANS Computations for David Taylor Model Body 1," NSWCCD-50-TR-2003/039, July, 2003.

de Kat, J. O. and Paulling, J. R., "The Simulation of Ship Motions and Capsizing in Severe Seas," *Trans. SNAME*, Vol. 97, pp. 139 – 168, 1989.

Deng, G. B. and Visonneau, M., 2000, "Comparison of Explicit Algebraic Stress Models and Second-Order Turbulence Closures for Steady Flows around the KVLCC2 Ship at Model and Full Scales,'' *Proc. Gothenburg 2000 A Workshop on Num. Ship Hydro.,* Goteborg, Sweden, 2000.

Ebert, M. P., Gorski, J. J., and Coleman, R. M., "Viscous Flow Calculations of Waterjet Propelled Ships," *Proc. 8th Int. Conf. on Numerical Ship Hydrodynamics*, Busan, Korea, Sept., 2003.

Frank, M. P., "The Physical Limits of Computation," *Computing in Science and Engineering,* pp. 16 – 26, May/June, 2002.

Froude, W. M., ``On Experiments with H.M.S. *Greyhound*,'' *Trans. INA*, Vol. 15, pp. 36 – 73, 1874.

Fung, S. C., O'Connell, L., and Forgach, K. M., "Resistance Performance Investigation of High-Beam Draft Large Size Displacement Hulls," *Proc. FAST' 2001*, Southampton, UK, Sept. 2001.

Gorski, J. J. "Drag Calculations of Unappended Bodies of Revolution," CRDKNSWC/HD-1362-07, May 1998.

Gorski, J. J., "Marine Vortices and Their Computation," *Proc. NATO RTO Applied Vehicle Technology Panel Symposium on Advanced Flow Management*, Loen, Norway, May, 2001.

Gorski, J. J., "Present State of Numerical Ship Hydrodynamics and Validation Experiments," *Journal Offshore Mechanics and Arctic Engineering*, Vol. 124, pp. 74-80, May 2002a.

Gorski, J. J., "A Perspective on the Role of RANS Codes for Predicting Large Amplitude Ship Motions," *Proc. 6th Int. Ship Stability Workshop*, Glen Cove, New York, Oct. 2002b.

Gorski, J. J. and Buley, G. M., ``Force and Moment Calculations of an Appendage Using the Reynolds Averaged Navier-Stokes Equations,'' CRDKNSWC/HD-1362-06, Jan., 1998.

Gorski, J. J. and Coleman, R. M., "Use of RANS Calculations in the Design of a Submarine Sail," *Proc. NATO RTO Applied Vehicle Technology Panel Spring 2002 Meeting*, Paris, France, April, 2002.

Gorski, J. J., Coleman, R. M., and Haussling, H. J., ``Computation of Incompressible Flow Around DARPA SUBOFF Bodies," DTRC Report No. 90/016, June, 1990.

Gorski, J. J., Haussling, H. J., Percival, A. S., Shaughnessy, J. J. and Buley, G. M., "The Use of a RANS Code in the Design and Analysis of a Naval Combatant," *Proc. 24th Symposium on Naval Hydrodynamics*, Fukuoka, Japan, July, 2002.

Gorski, J. J., Miller, R. W., and Coleman, R. M., "An Investigation of Propeller Inflow for Naval Surface Combatants," *Proc. 25th Symposium on Naval Hydrodynamics*, St. John's, Newfoundland and Labrador, Canada, August, 2004.

Himeno, Y., "Prediction of Ship Roll Damping – State of the Art," Report 239, Dept. of Naval Arch. and Marine Eng., Univ. of Michigan, 1981.

Hoerner, S. F., "Fluid-Dynamic Drag," Published by the author, Brick Town, NJ, 1965.

Hyams, D.G., Sreenivas, K., Sheng, C., Briley, W.R., Marcum, D.L., and Whitfield, D.L., "An Investigation of Parallel Implicit Solution Algorithms for Incompressible Flows on Multielement Unstructured Topologies," *AIAA Paper 2000-0271*, 38th Aerospace Sciences Meeting, Reno, NV, Jan., 2000.

ITTC, ``Report of the Resistance and Flow Committee,'' *Proc. 21st ITTC*, Trondheim, Norway, 1996.

ITTC, "The Manoeuvering Committee Final Report and Recommendations to the 22nd ITTC," *Proc. 22nd ITTC*, Seoul Korea & Shanghai China, Sept. 1999.

Jameson, A., "The Role of CFD in Preliminary Aerospace Design," FEDSM2003-45812, *Proc. FEDSM'03*, Honolulu, Hawaii, July, 2003.

Jameson, A., Sriram, Martinelli, L, and Haimes, B., "Aerodynamic Shape Optimization of Complete Aircraft Configurations using Unstructured Grids," AIAA Paper No. 2004-533, 2004.

Kaplan, P., Ankudinov, V., and Jakobsen, B. K., "Modular Mathematical Models for Ship Maneuvering," SNAME Tech. & Research Report NO. 56, 2002.

Kim, K-H., "Unsteady RANS Simulation for Surface Ship Dynamics," *DoD HPCMP Users Group Conf.*, Biloxi, MS, June, 2001.

Kim, S.-E., "Reynolds Stress Transport Modeling of Turbulent Shear Flow Past a Modern VLCC Hull Form,'' *Proc. Gothenburg 2000 A Workshop on Num. Ship Hydro.*, Goteborg, Sweden, 2000.

Krueger, K. E., Gorski, J. J., and Miller, R. W., "Appendage Alignment Using RANS-Based Numerical Methods," NSWCCD-50-TR-2002/035, Nov., 2002.

Larrson, L., Stern, F., and Bertram, V., "Benchmarking of Computational Fluid Dynamics for Ship Flows: The Gothenburg 2000 Workshop," *Journal of Ship Research*, Vol. 47, No. 1, pp. 63-81, March, 2003.

Metcalf, B. J., Grabeel, J. A., Karafiath, G., Hendrix, D., and Noblesse, F. L., "Rapid Resistance Evaluation of High-Speed Ships," Naval Surface Warfare Center, Carderock Division, Technical Digest, pp. 31-43, April, 2004.

Miller, R. W., Gorski, J. J., and Fry, D. J., "Viscous Roll Predictions of a Circular Cylinder with Bilge Keels," *Proc. 24th Symposium on Naval Hydrodynamics*, Fukuoka, Japan, July, 2002.

NSWCCD, "High-Speed Sealift Technology Development Plan," NSWCCD-20-TR-2002/06, May, 2002.

Patel, V. C., "Perspective: Flow at High Reynolds Number and Over Rough Surfaces – Achilles Heel of CFD,'' *Journal of Fluids Engineering*, Vol. 120, pp. 434 – 444, 1998.

Paterson, E.G., R. Wilson, and F. Stern, "General Purpose Parallel Unsteady RANS for Ship Hydrodynamics," *Computers and Fluids*, June, 2000.

Perić, M., "Computation of Engineering Flows," *Ship Technology Research*, Vol. 41, pp. 204 – 214, 1994.

Ratcliffe, T., "Validation of Free Surface Reynold's Averaged Navier-Stokes and Potential Flow Codes,'' *Proc. 22nd Symposium Naval Hydrodynamics*, Washington D. C., pp. 964 – 980, 1998.

Rood, E. P., "Computational Ship Hydrodynamics for Revolutionary Naval Combatants,'' *DoD HPC User's Group Conf.*, Albuquerque, NM, 2000.

Schütte, A., Einarsson, G., Madrane, A., Schöning, B., Mönnich, W., and Krüger, W.-R., "Numerical Simulation of Maneuvering Aircraft by Aerodynamic and Flight-Mechanic Coupling," *Proc., NATO RTO AVT Symp.*, Paris, France, 2002.

Scragg, C. A., Reed, A. M., Wyatt, D. C., and Ratcliffe, T. J., "Hull Form Development of the *Sea Shadow* and Applications of the Technology to Monohulls," *Trans. SNAME*, Vol. 106, pp. 443 – 483, 1998.

Sheridan, D., et al., "The ASSET Program – A Current Navy Initiative," *SNAME STAR Symp.*, Paper 1-A-33, 1984.

Taylor, L. K. and D. L. Whitfield, "Unsteady Three-Dimensional Incompressible Euler and Navier-Stokes Solver for Stationary and Dynamic Grids," AIAA Paper No. 91-1650, June, 1991.

Taylor, L. K., A. Arabshahi, and D. L. Whitfield, "Unsteady Three-Dimensional Incompressible Navier-Stokes Computations for a Prolate Spheroid Undergoing Time-Dependent Maneuvers," AIAA Paper No. 95-0313, Jan., 1995.

Taylor, L., K., ., Pankajakshan, M., Jiang, M., Sheng, C., Briley, W. R., Whitfield, D. L., Davoudzadeh, F., Boger, D. A., Gibeling, H. J., Gorski, J. J., Haussling, H., Coleman, R., and Buley, G. "Large-Scale Simulations for Maneuvering Submarines and Propulsors," AIAA Paper No. 98-2930, 1998.

Van, S. H., Kim, W. J., Kim, H. R., and Lee, S. J., "Wind Tunnel Test on Flow Characteristics of KRISO 300K VLCC Double Model," *Proc. Japan-Korea Joint Workshop on Marine Hydro.*, Fukuoka, Japan, 1999.

INITIAL DISTRIBUTION

NAVSEA

Code	**Name**
PEO Ships	
PMS 500	
PMS 501	
SEA 05	
05D	(Czapiewski, Reynolds)
05H	(Nix, Crockett, King, Schumann, Stout, Waters)
05Z9	(Tsao)
NSWC Technical Director	(Giacchi)
Ships & Ship Systems PAD	(Reeves)
Littoral Warfare Systems PAD	(Skinner)

ONR

Code	**Name**
Technical Director	(Lubard)
Chief of Staff	(Lowell)
ACNR	(Kamp)
Chief Scientist	(Walker)
33	(Pohanka)
33X	(Littlefield)
33	(Carlin, Joslin, Kim, Ng, Muench, Purtell, Webster)

DARPA (Porter)

DDR&E (Lekoudis)

NUWC

Chief Technology Officer (Nadolink)

NG (Hamadyke, Preisel, Weinrich)

EB (Panosky)

ANTEON (Hazen, Kingsley, Shaughnessy)

CDI Marine (Lavis)

DTIC

CENTER DISTRIBUTION

Code	Name
001	(Beach)
002	(Corrado)
0021	(Barkyoumb)
0022	(Teter)
0023	(Byers)
20	(Wade)
2101	(Merryman)
2420	(Fung, Kennell)
2820	(Offutt)
5010	Administrative Office
5030	(Jessup)
5050	(Reed)
5060	(Walden)
5080	(Cox)
5200	(Day, Hendrix, Karafiath, Noblesse)
5300	(Coakley, Ebner)
5400	(Szwerc, Black, Coleman, Dai, Ebert, Gorski, Lee, Miller, Scherer, Shen, Slomski, Telste, Wilson)
5500	(Applebee, Belknap, Becnel, Campbell, Hoyt, Odea)
5600	(Ammeen, Fu)
7051	(Blake)
7204	(Farabee)
91	(Fry, Moss)